Summer 8-11-2015

Comparative Analysis of Load Flow Techniques for Steady State Loading Margin and Voltage Stability Improvement of Power Systems

Santosh Togiti
University of New Orleans, stogiti@uno.edu

Comparative Analysis of Load Flow Techniques for Steady State Loading Margin And Voltage Stability Improvement of Power Systems

A Thesis

Submitted to the Graduate Faculty of the
University of New Orleans
in partial fulfillment of the
requirements for the degree of

Master of Science
in
Engineering
Electrical Engineering

by

Santosh K Togiti
B.E, Osmania University, 2010

August 2015

To my mother,
Leelavathi

Acknowledgements

I would like to convey my deepest gratitude to my research advisor, Dr. Ittiphong Leevongwat and my academic advisor Dr. Parviz Rastgoufard for their constant support in helping me conduct and complete this work, without whose guidance this thesis would not have been possible. They have been a great source of inspiration and knowledge whose direction has helped me begin and conclude this investigation.

I would like to thank my committee member Dr. Ebrahim Amiri for his valuable feedback on my work.

I would like to thank my brother Varun Togiti, for his never ending support and encouragement. And for his invaluable insight which lead me to where I am today. Last but not least, I would like to thank my family and friends for their support and encouragement.

Contents

List of Figures

List of Tables

Abstract

Installation of reactive compensators is widely used for improving power system voltage stability. Reactive compensation also improves the system loading margin resulting in more stable and reliable operation. The improvements in system performance are highly dependent on the location where the reactive compensation is placed in the system. This paper compares three load flow analysis methods - PV curve analysis, QV sensitivity analysis, and Continuation Load Flow - in identifying system weak buses for placing reactive compensation. The methods are applied to three IEEE test systems, including modified IEEE 14-bus system, IEEE 30-bus system, and IEEE 57-bus system. Locations of reactive compensation and corresponding improvements in loading margin and voltages in each test system obtained by the three methods are compared. The author also analyzes the test systems to locate the optimal placement of reactive compensation that yields the maximum loading margin. The results when compared with brute force placement of reactive compensation show the relationship between effectiveness of the three methods and topology of the test systems.

Keywords: Reactive Power, Static Voltage Stability, Placement, Load Flow Analysis, Comparative Analysis

1 Introduction

This chapter provides an overview of the evolution and establishment of modern power systems. Various aspects of power systems including load flow techniques, voltage stability, voltage stability analysis techniques, and loading margin in particular are introduced. A historical review of voltage stability analysis of power systems and methods of voltage stability analysis are presented. This thesis presents a comparative analysis of techniques in load flow analysis for steady state voltage stability and loading margin improvements.

The remainder of this chapter includes an overview of modern power systems in subsection 1.1, power system stability in subsection 1.2, voltage stability of power system in subsection 1.3, voltage stability analysis methods in subsection 1.4, and practical techniques for prevention of voltage collapse in subsection 1.5. The specific scope of this thesis is represented in subsection 1.7 after providing a historical review of major blackouts caused by voltage instability in subsection 1.6.

1.1 Modern Power Systems

The commercial use of electricity began in the late 1870s when arc lamps were used for lighthouse illumination and street lighting [1]. The first complete electric power system (comprising a generator, cable, fuse, meter, and loads) was built by Thomas Edison - the historic Pearl Street Station in New York City which began operating in September 1882. The load, which consisted entirely of incandescent lamps, was supplied at 110 V through an underground cable system. Within few years similar systems were in operation in most large cities throughout the world. With the development of motors by Frank Sprague in 1884,

motor loads were added to such systems.

Initially, dc systems were widely spread but by 1886 were completely superseded by ac systems. The reason being the increasingly apparent limitations of dc systems. DC systems could deliver power only a short distance from the generators. To keep transmission losses (I^2R) and voltage drops to acceptable levels, voltages had to be high for long-distance power transmission. Such high voltages were not acceptable for generation and consumption of power, therefore a convenient means for voltage transformation became a necessity. Some of the main reasons for the transition from dc to ac systems are easy transformation of voltages thus providing the flexibility for use of different voltages for generation, transmission, and distribution, AC generators are much simpler than dc generators, and AC motors are much simpler and cheaper than dc motors.

The decision to choose ac at Niagara Falls to transmit power about 30 km away to Buffalo ended the ac versus dc controversy and established victory for the ac systems. In early period of ac power transmission, frequency was not standardized. The use of many different frequencies posed problems for interconnection. So eventually 60 Hz was adopted as standard in North America, many other countries selected 50 Hz. The increasing need for transmitting large amounts of power over longer distances created an incentive to use progressively higher voltage levels. To avoid the proliferation of an unlimited number of voltages, the industry has standardized voltage levels. The standards are 115, 138, 161, 230 KV for high voltage (HV) class, and 345, 500 and 765 KV for the extra-high voltage (EHV) class [1].

Interconnection of neighboring utilities leads to improved security and economy of operation due to the mutual assistance that the utilities can provide. Several benefits

including the ones described above have been recognized from the beginning and interconnections continue to grow leading to todays one big complex interconnected system with almost all the utilities in United States and Canada. The design and secure operation of such a system are indeed challenging problems.

In recent years, power demands around the world generally and particularly in North America have experienced rapid increase due to the increase of customers' requirements. The report from Renewable Energy Transmission Company (RETCO) [2] about the infrastructure situation of U.S. electric grids states that electricity consumption accounts for 40% of all energy consumed in the U.S. and the electricity demand grows significantly and it will reach an increase rate of 26% by 2030.

Since 1982, growth in peak demand for electricity has exceeded transmission growth by almost 25% every year. Yet spending on research and development is the lowest of all industries [3]. Even with increase in demand, there has been chronic underinvestment in getting energy where it needs to go through transmission and distribution which limits grid efficiency and reliability. Since 2000, only 668 additional miles of interstate transmission have been built [3]. As a result, system constraints worsen at a time when outages and power quality issues are estimated to cost American business more than $100 billion on average each year. Under these extreme conditions, the need for maintaining stable operation of the grid is most important.

1.2 Power System Stability

Reference [4] defines power system stability as "the ability of an electric power system, for a given initial operating condition, to regain a state of operating equilibrium after being subjected to a physical disturbance, with most system variables bounded so that

practically the entire system remains intact" . This definition applies to an interconnected power system as a whole where the stability of a particular generator or a group of generators is of interest. A remote generator may lose synchronism without causing cascading instability of the whole system. Similarly, stability of particular loads or load areas may be of interest.

The power system is a highly nonlinear system that operates in a constantly changing environment; loads, generator outputs and key operating parameters change continually. When subjected to a disturbance, the stability of the power system depends on the initial conditions and nature of the disturbance. Power systems are subjected to a wide range of disturbances, small and large. Small disturbances in the form of load changes occur continually; the system must be able to adjust to the changing conditions and operate satisfactorily. It must also be able to survive numerous disturbances of a severe nature, such as a short circuit on a transmission line or loss of a large generator. A large disturbance may lead to structural changes due to the isolation of the faulted elements.

However, it is impractical and uneconomical to design power system to be stable for every possible disturbance [4]. The design contingencies are selected on the basis that they have a reasonably high probability of occurrence. A stable equilibrium set thus has a finite region of attraction; the larger the region, the more robust the system with respect to large disturbances. The region of attraction changes continually with changes in operating conditions of the power system.

Power system stability is a high dimensional and complex problem and in order to deal with different types of instabilities occurring in the system it helps to make simplifying assumptions to analyze specific types of problems using an appropriate degree of detail system representation and appropriate analytical techniques. The understanding of

stability problem is greatly facilitated by the classification of stability into various categories [1]. The power system stability is mainly divided into rotor angle stability, frequency stability and voltage stability. Voltage stability is explained in detail in subsequent sections as it is the main focus of this thesis.

1.3 Voltage stability of Power System

Voltage stability is the ability of a power system to maintain steady acceptable voltages at all buses in the system under normal operating conditions and after being subjected to a disturbance [1]. A system enters voltage instability when a disturbance, increase in load demand, or change in system condition causes a progressive and uncontrollable drop in voltage. The main factor causing instability is the inability of the power system to meet the demand for reactive power. A possible outcome of voltage instability is the loss of load in an area, or tripping of transmission lines and other elements by their protective systems leading to cascading outages. Voltage collapse is the process by which the sequence of events accompanying voltage instability leads to a blackout or abnormally low voltages in a significant part of the power system.

Voltage instability is mainly caused because of the loads; after a disturbance, power consumed by the loads tends to be restored by the action of voltage regulators, tap changing transformers, and thermostats. Restored loads increase the stress on high voltage network by increasing the reactive power consumption and causing further voltage reduction. A run-down situation causing voltage instability occurs when load dynamics attempt to restore power consumption beyond the capability of transmission network and the connected generation [1] [5].

There is also a risk of overvoltage instability in the system which has been

experienced at least once [6]. This is caused by the capacitive behavior of the network as well as by under excitation limiters preventing generators and/or synchronous compensators from absorbing the excess reactive power. This instability is associated with instability of the combined generation and transmission system to operate below some load level.

Voltage stability problems may also be experienced at HVDC links [7]. They are usually associated with HVDC links connected to weak ac systems and may occur at rectifier or inverter stations, and are associated with the unfavorable reactive power "load" characteristics of the converters. The HVDC link control strategies have a significant influence on such problems, since the active and reactive power at the ac/dc junction are determined by the controls. If the resulting loading on the ac transmission is relatively with the time frame of interest being in order of one second or less.

It is useful to classify voltage stability into sub categories as discussed below:

1. *Large - disturbance voltage stability* is the ability of the system to maintain steady permissible voltages following large disturbances such as system faults, generator trips or other circuit contingencies. This phenomenon is affected by the system and load characteristics, and the interactions of both continuous and discrete controls and protections. Determination of large signal voltage stability requires the examination of the nonlinear response of the power system over a period of time sufficient to capture the performance and interactions of devices such as motors, under load tap changers, generator field current limiters, and speed governors. The study period of interest may extend from a few seconds to tens of minutes. Therefore, long-term dynamic simulations are required for analysis.

2. *Small - disturbance voltage stability* is the ability of the power system to maintain steady

permissible voltages when subjected to small perturbations such as incremental changes in system load. This form of stability is influenced by the characteristics of the load, continuous controls, and discrete controls at a given instant of time. This concept is useful in determining, at any instant, how the system responds to small system changes. To identify the factors influencing stability, system equations can be linearized for the analysis with appropriate assumptions.

The time frame of interest for voltage stability problems may vary from a few seconds to tens of minutes. Therefore, voltage stability can be classified into short term and long term on this basis.

1. *Short - term voltage stability* involves dynamics of fast acting load components such as induction motors, electronically controlled loads, and HVDC converters. The study period of interest is in order of several seconds, and the analysis requires solution of appropriate system differential equations [4]. This analysis needs dynamic modeling of loads.

2. *Long - term voltage stability* involves slower acting equipment such as tap-changing transformers, thermostatically controlled loads, and generator and current limiters. This analysis assumes that inter - machine synchronizing power oscillations have dumped out, resulting in a uniform system frequency [8]. The focus is on slower and longer duration phenomena that accompany large scale system upsets and on the resulting large, sustained mismatches between the generation and consumption of active and reactive powers. Long - term stability is usually concerned with system disturbances that involve contingencies beyond the normal system design criteria.

1.4 Methods of Voltage Stability Analysis

Voltage stability problems normally occur in heavily stressed systems. While the disturbance leading to voltage collapse may be initiated by a variety of causes, the underlying problem is a inherent weakness in the power system. The main factors other than the design limitations of the system are generator reactive power/voltage control limits, load characteristics, characteristics of reactive compensations devices, and the action of voltage control devices such as under load tap changing transformers (ULTCs) [1].

The voltage stability analysis for a given system state involves the examination of two concepts [9]:

1. *Proximity to Voltage Instability:* A measure of how close the system is to voltage instability. Physical quantities such as load levels, active power flow through critical interface and reactive power reserve can be used to measure the distance to instability. The most appropriate measure for a given situation depends on the specific system and the intended use of the margin. Considerations must be given to possible contingencies such as line outages, loss of generating units or reactive power sources, etc.,

2. *Mechanism of Voltage Instability:* This includes the determination of the cause of instability including the key factors, voltage - weak areas and also finding out the measures to improve stability.

The voltage instability problem is solved by many different methods, which can be distinguished mainly in two groups: static and dynamic methods. Dynamic methods apply real - time simulation in time domain using precise dynamic models for all instruments in a power system. It shows the time domain events and their characteristic curves which

eventually lead the system into voltage collapse. These methods mainly depend on the solutions of large sets of differential equations created to describe the model characteristics of electrical devices and their internal connections. Dynamic simulation is particularly effective for detailed study of specific voltage collapse situations and coordination of protection and time dependent action of controls. The dynamic simulation of large-scale power system is time consuming and relies heavily on the computer's performance.

The system dynamics influencing voltage instability are usually slow. Therefore, static methods can be used to analyze many aspects of the problem. The static analysis techniques allow examination of a wide range of system conditions and, if appropriately used, can provide much insight into the nature of the problem and identify the key contributing factors.

Static Analysis captures snapshots of system conditions at various time frames along the time-domain trajectory. The electric utility industry has been widely dependent on conventional power-flow techniques for static analysis of voltage stability. V-P and V-Q curves are the most commonly used methods for voltage stability analysis. Although these methods involve the establishment of stability characteristics by unrealistically stressing each individual bus in the system. As a consequence, several techniques have been proposed for voltage stability analysis using the static approach.

F. D. Galiana proposed a novel technique based on concept called the load flow feasibility region (FR) and the steady state stability or feasibility margin (FM) [10]. The method does not rely on load flow solutions to give an estimate of how close the bus injection vectors (P, Q, or V^2) are to the boundary of FR thus avoiding the problems of non-convergence under the system loading limits. The FR is the set of generalized bus injections

and the FM is a scalar ranging from 0 and 1. FM is a measure of the angle between the bus injection vector and the closest injection vector on the the boundary of the FR along some specified direction. A value of FM equal to 0 implies that the injections are on the boundary of the FR and a value of FM greater than 0 indicates that the injections are inside the FR.

B. Gao, G. K. Morris, P. Kundur presented a technique to analyze the voltage stability of large power systems using modal analysis technique [9]. The method computes a specified number of the smallest eigenvalues and the associated eigen vectors of a reduced Jacobian matrix and the associated bus, branch and generation participation factors. The magnitude of the eigen values, each of which is associated with a mode of voltage/reactive power variation determines the degree of stability of the i^{th} modal voltage. The smaller the eigen value, closer the mode is to instability. The eigenvectors are used to describe the mode shape and to information about the network elements and generators which participate in each mode. The magnitude of eigen values provides a relative measure to instability. However, they do not provide an absolute measure because of the nonlinearity of the problem [1]. At any given operating condition, the system is stressed incrementally until it becomes unstable to obtain a MW distance to instability. Modal analysis is then applied at each operating point which gives the information about how stable the system is and how much extra load the system can take. At the system's voltage stability critical point, modal analysis helps identify the voltage stability critical areas and elements participating in each mode.

The relation between voltage instability and multiple load flow solutions has been investigated by Y. Tamura [11]. A set of N criteria are preset to differentiate between the solution pair of the load flow to identify the stable and unstable one. The criterion used in this discussion are sign of Jacobian determinant in the load flow calculation, load flow sensitivity

for node injections and system parameters, and increase or decrease of stored energy of the elements L and C in the electric power system due to small frequency disturbance raise. Although the criterion 1 has some disadvantages in that it needs Jacobian J in the stable system and involves uncertainty of sign{det J} when the even number of the eigenvalues vary to the unstable mode, in the criteria 2 and 3 the property of solution can be judged at any time point without the prior information.

The QV curve method [1], [27] has been used as a planning tool by many utilities. QV curve may help engineers to identify critical buses in the system as well as the reactive power injections needed at those buses to ensure voltage security. Pablo Guimaraes, Ubaldo Fernandez, Tito Ocariz, Fritz W. Mohn, A. C. Zambroni de Souza presented a work where they used QV and PV curves as planning tools of analysis [28]. In this work, a planning tool based on some voltage stability criteria is proposed. They employed tangent vectors to identify citical buses in the system and QV curves to identify the buses with least and larger reactive power to obtain a good planning strategy. QV sensibility and curves have been employed for voltage stability assessment [29], [30] in other power system studies.

V-Q sensitivity analysis has advantage that it provides voltage stability-related information from a system-wide perspective and clearly identifies areas that have potential problems. The elements of the Jacobian matrix gives the sensitivity between power flow and bus voltage changes. The V-Q sensitivity at a bus represents the slope of the Q-V curve at the given operating point. A positive V-Q sensitivity is indicative of stable operating, the smaller the sensitivity, the more stable the system. As stability decreases, the magnitude of the sensitivity increases, becoming infinity at the stability limit. A negative V-Q sensitivity is indicative of unstable operation, even a small negative sensitivity represents a very unstable

operation [1]. A detailed mathematical description of Q-V sensitivity is given in further chapters.

The PV curves represent the voltage variation with respect to the variation of load active power. They are produced by a series of load flow solutions for different load levels uniformly distributed, by keeping constant power factor. The active power is proportionally incremented to the participating factors of each generator. PV curves are widely used in industry for static voltage stability analysis of power system. The PV curves are plotted for each bus and the bus which reaches the stability margin is identified as the weak bus. A detailed mathematical description of the PV curves and how they are derived is given in further chapters. S. Corsi and G. N. Taranto presented a paper elaborating the understanding of dependence of the shape of the "nose" of a Power-Voltage (PV) curve in a EHV bus, by the power system dynamics [13]. The paper showed in detail the involvement of control loops in voltage instability phenomenon and their effect on the shape of PV curve.

Venkataraman Ajjarapu, Colin Christy presented a method of finding a continuum of power flow solutions starting at some base load and leading to the steady state stability limit (critical point) of the system [12]. The method uses reformulated power flow equations with a load parameter as an additional parameter. The continuation algorithm is then applied to the system of reformulated power flow equations. The process involves predictor and corrector steps to find the consecutive solutions, it remains well conditioned near and beyond the stability limit consequently avoiding the problems of conventional power-flow which are prone to convergence problems at operating condition near the stability limit. A detailed mathematical description of the method is given in further chapters.

Ana Claudia M. Valle presented the use of tangent vectors for voltage collapse

analysis [24] where the system tangent vectors were computed using inverse of the Jacobian matrix. In this work, normalized tangent vectors were compared to the eigenvectors to whom the same normalization was applied. A. C. M. Valle later presented a paper where he used tangent vectors and eignevectors in power system voltage collapse analysis [25]. In this work, a relation between the tangent vectors and eigenvectors is used to converge to the bifurcation point sooner and to identify the most sensible bus and the generator which most influence the bus voltage oscillation.

B. Isaias Lima Lopes, A. C. Zambroni de Souza, and P. Paulo C. Mendes presented a paper that talked about the use of tangent vectors as a tool for voltage collapse analysis considering a dynamic model [26]. In this work, they employed the continuation method for the power flow model to calculate the indices for each operating point and the process is repeated for dynamic system model. The results are compared and showed that dynamic model may be more pessimistic for loading margin evaluation, since the static model tends to produce results more conservative. They conclude that monitoring the indices during the system load increase may not be enough to identify the voltage collapse point. However, tangent vector presents a better behavior than the least eigenvalue, since latter is associated with a sudden variation at the voltage collapse point.

Continuation load flow has been used in several instances for steady state power system analyses and to obtain system tangent vectors [28] [31] [32] [33]. A. Sode-Yome, N. Mithulananthan, K. Y. Lee presented a paper comparing various FACTS devices [14]. They used several performance measures including PV curves, voltage profiles, and power losses are compared to evaluate their performance. Continuation load flow was used for steady state analysis to identify weak bus of the system to install reactive compensation. The

paper investigates both placement and sizing techniques for better choice of FACTS devices for enhancing loading margin and static voltage stability.

1.5 Practical Techniques for Prevention of Voltage Collapse

Several measure could be taken to avoid voltage collapse, system design measures and system operating measures are the common practices for this purpose [1]. System design measures that can be taken to avoid voltage collapse are:

1. **Application of Reactive Power-Compensating devices:** Adequate stability margins should be maintained by selecting the appropriate sizes, ratings, and locations for reactive compensation devices based on detailed studies covering the most onerous system conditions for which the system is required to operate satisfactorily

2. **Control of Network Voltage and Generator Reactive output:** Generator AVR regulates voltages on the high-tension side of the step-up transformer moving the point of constant voltage electrically closer to the loads. A secondary outer control loop with response time of about 10 seconds is used to regulate network side voltage.

3. **Coordination of Protections/Controls:** Lack of coordination between equipment protections/controls and power system requirements could lead to voltage collapse, adequate coordination should be ensured based on dynamic simulation studies. Adequate control measures should be provided for relieving any overload conditions before isolating equipment from the system, tripping of equipment should be the last resort to prevent an overloaded condition.

4. **Control of Transformer Tap Changers:** Tap changing transformers are used to reduce the risk of voltage collapse. Strategies developed based on knowledge of the load

and distribution system characteristics must be employed to improve ULTC control [1]. Microprocessor-based ULTCs on the other hand provide unlimited flexibility in implementing control strategies so as to take advantage of the load characteristics.

5. **Undervoltage Load Shedding:** Load shedding based on carefully designed schemes to cater unplanned or extreme situations is a low cost means of preventing widespread system collapse. It is employed in both underfrequency and undervoltage control, the characteristics and locations of loads to be shed are more important for voltage problems than they are for frequency problems [1].

System-operating measure that can be taken to avoid voltage collapse are:

1. **Stability Margin:** Maintaining adequate voltage stability margin by scheduling of reactive power and voltage profiles could help avoid voltage collapse. All systems are different and should be the parameters and degree of margin designed based on the particular system.

2. **Spinning Reserve:** Maintaining adequate spinning reserves and switching in capacitors by appropriately identifying the need to maintain the desired voltage profile.

3. **Operators' Action:** Operators must be able to identify voltage stability-related symptoms and take remedial actions based on well designed strategies to prevent voltage collapse. On-line monitoring and analysis could direct to appropriate preventive actions so as to avoid voltage collapse situation.

1.6 Major Blackouts caused by Voltage Instability

Power industries were initially dedicated as service oriented and driven completely by government. Gradually as the system became large with increasing demand,

deregulation was introduced to improve the managerial efficiency. This lead to a competitive market structure with increase in system utilization and it also increased the risk on system operations by stressing the power systems and reducing the predictability of operations. Interconnection with neighboring countries or sub systems made the network stronger, however this also increases the area covered by the network thus increasing risk on external interferences. This also increases the risk of having many disturbances at the same time therefore makes it difficult to design the system to sustain N-1 contingency and reduce the security of the power system.

The first officially reported major blackout was the Northeast power failure on 9^{th} November 1965. The backup protection tripped one of the five line connecting the northeast and southwest under heavily loaded conditions [15]. This eventually led to the tripping of rest of the four lines diverting 1700 MW of power which eventually led to total system collapse. It was also identified that there was not enough spinning reserve kept at the time the blackout was initiated. The blackout affected 30 million people and New York City was in darkness for 13 hours. The 13^{th} July 1977 collapse of Con Edison System left 8 million people in darkness, including New York City for periods from 5 to 25 hours [15]. Lack of preparation for major emergencies, operating errors, questionable system design, and equipment malfunction with a combination of natural events were recognized as the causes of the event. Imperfect operation of protective equipment resulted in three of four lines tripping which resulted in transmission ties overloading eventually opening them which led to total system operation failure.

On 23^{rd} July 1987, a power failure occurred in Tokyo, Japan due to insufficient reserve. There was an outage of 3.4 GW power out of the maximum power demand of 38.5

GW, the 1.52 GW reserve was insufficient for the unusual high peak demand due to extreme hot weather [15]. Widely used constant power characteristic loads such as air conditioners reduced the network voltage rapidly and caused dynamic voltage instability. The Western North American power system reported an interruption leading to failure on 2^{nd} July 1996. It was initiated with a flashover to a tree which created a short circuit on a transmission line causing a 2 GW power interruption. This line was a series compensated with a capacitor, the loss of power transfer caused voltage depression and thus tripped a few hydro generators due to high field current causing a voltage decay. To prevent further down process, five islanded sub systems were formed with controlled and uncontrolled load shedding.

50 million people were affected on 14^{th} August 2003 in US and Canadian due to a blackout which interrupted 63 GW load. In this event 400 transmission lines and 531 generating units at 261 power plants tripped. The major reason was found to be insufficient reactive power, which lead to voltage instability. Failure was initiated with tripping voltage regulator due to over excitation and when the operators tried to restore the regulators, generators which were generating high reactive power were tripped. Finally, tripping of a tie line lead to cascading blackout of the entire region. Several other blackouts were reported over the past decade including 23^{rd} September 2003 blackout in Europe, the Swedish/Danish system, 28^{th} September 2003 blackout in Italy, and a major interruption in Victoria, Australia on 16^{th} January 2007 that interrupted service to 480,000 customers.

Operator action and load shedding could have greatly reduced the impact in most of the situations listed above [15]. Gathering and analysis of technical information on the root cause of blackouts, development of load shedding schemes with technical explanation, a detailed study about the restoration problems with critical study, and exclusive focus

on requirement of the system operator's training are few of the measures that could avoid a system wide blackout.

1.7 Scope and Contribution of Thesis

Over the years, various methods have been used to identify the weak buses of a system for reactive power installation in several studies. This thesis is an investigation into whether there are any differences in improvement of the system design and consequently performance caused by the use of different load flow analysis techniques to identify the location for installing reactive compensation. The investigation conducted in this thesis consists of comparing three methods namely Continuation Load Flow, PV Curve Analysis, and QV sensitivity analysis to identify the weak buses in multiple systems and a reactive compensation is installed at these locations. Various metrics including maximum loading margin and the system differential active and reactive power losses are compared to the results of installing a reactive compensation at the optimal location obtained from brute-force to identify the method(s) that identifies a location that gives better results compared to other method(s).

Load flow equations are multi dimensional and coupled set of equations, which usually are solved using iterative techniques. Several techniques have been developed for this purpose and the results obtained are analyzed using even more techniques. PV curve analysis and QV sensitivity analysis are obtained from the traditional load flow. Continuation load flow is more recent developed method of load flow analysis which gives other sensitivity information useful in system analysis.

PV curves are the plots of real power and voltage at some critical buses which help determine the static voltage stability of the system. For any given loading condition the bus voltage has two possible values except at the stability limit where the load flow equations do not converge. One of these two is in stable operating mode and the other one is not. It

is of utmost importance to never operate the system at unstable voltage levels, this could cause a serious black out though uncontrollable collapse of voltage levels in the system. PV curves help identify the operating voltages for different levels of real power requirement and also specify the weak buses in the system which are prone to voltage instability.

QV sensitivity analysis is the change in bus voltage with injection or absorption of reactive power (Q) at any bus. For a system to be in stable operating mode, it is necessary that all the buses in the system have a positive QV sensitivity. The degree of sensitivity can be observed in the elements of the Jacobian matrix of load flow equations. For a given set of parameters ($P, Q, V and \theta$), the magnitude of elements of the Jacobian matrix identify the buses that are highly sensitive to Q. The small the QV sensitivity, the more stable the bus is. As the stability decreases, the magnitude of QV sensitivity increases becoming infinite at stability limit. However, even a small negative QV sensitivity is an indicative of highly unstable operation.

Continuation load can be used to compute the load flow solutions beyond the stability limit of the system which conventional load flow techniques fail to provide. This is due to the convergence problems of the Jacobian matrix in conventional load flow methods, which the Continuation load flow method over comes by employing a prediction and correction of tangent vectors at a given solution of the load flow equations. The method provides very useful sensitivity information at no additional cost at all. The magnitudes of the tangent vectors at a given solution provide the sensitivity information of all the buses. The greater the magnitude, the more unstable the bus is in the system.

Reactive power installation is a widely used technique for voltage stability and loading margin improvement of the system. The location for reactive power installation

plays a crucial role in determining the improvement that can be obtained in the system. Installation of reactive compensation at weak buses of the system has shown to improve the system voltage stability and loading margin [14]. However, the definition of a weak bus changes with the load flow and sensitivity analysis used. Thus, it is important to identify the differences in improvement of system performance based on the analysis method employed.

The measure of improvement in system performance is an important aspect for analysis purposes. Several metrics could be used to achieve this purpose. Differential real and reactive power losses of the system and maximum loading margin of the system are the metrics used in this thesis to measure the system performance.

The active and reactive power losses are related to the bus voltage angle and magnitude stability of the system. It can be observed from the system Jacobian matrix that the voltage angle is dependent on the real power available at a bus and the voltage magnitude is dependent on the reactive power available at a bus. Reducing the losses increases the available real and reactive power at a bus, thus improving the voltage stability.

Maximum loading margin of a system is the load beyond which increase in load will drive the system to instability. The system is operated by maintaining sufficient margin from this maximum loading margin so as to always keep the system in stable operating conditions. An increase in the system maximum loading margin will provide an improvement in the load which the system can supply and still keep a sufficient margin from the maximum loading margin.

In further chapters, various load flow methods, analysis techniques, and metrics that will be used in this thesis will be discussed in detail. Then methodology is proposed for comparing the improvement of system performance based on location of reactive power

installation. The methodology is then applied to various test systems and the results are presented. Conclusions are then drawn based on the simulation results obtained.

2 Mathematical Modeling

Mathematical modeling of the load flow problem, various load flow analysis techniques along with stability analysis techniques are discussed in this chapter.

2.1 Load Flow Problem

The main objective of solving the load flow problem is calculation of the power flows and voltages of a transmission network for specified bus conditions. These calculations are required for both steady state and dynamic analysis as well. The bus classification are as described below:

1. **Variables:** Voltage magnitude, Voltage phase angle, real power requirement, and reactive power requirement.
2. **Voltage-Controlled (PV) bus:** Voltage magnitude and active power are known quantities for this kind of buses, reactive power limits are specified as well.
3. **Load (PQ) bus:** Active and reactive power requirements are the known quantities at this type of bus locations.
4. **Slack (Swing) bus:** Voltage magnitude and phase angle are the known quantities for this type of bus, there must be at least one bus with unspecified P and Q because of the unknown P and Q losses in the system.

The network equations in terms of the node admittance matrix are written as follows:

$$\begin{bmatrix} \tilde{I}_1 \\ \tilde{I}_2 \\ \tilde{I}_3 \\ \vdots \\ \tilde{I}_n \end{bmatrix} = \begin{bmatrix} Y_{11} & Y_{12} & Y_{13} & \dots & Y_{1n} \\ Y_{12} & Y_{22} & Y_{23} & \dots & Y_{2n} \\ Y_{31} & Y_{32} & Y_{33} & \dots & Y_{3n} \\ \vdots & \vdots & \vdots & \ddots & \vdots \\ Y_{n1} & Y_{n2} & Y_{n3} & \dots & Y_{nn} \end{bmatrix} \begin{bmatrix} \tilde{V}_1 \\ \tilde{V}_2 \\ \tilde{V}_3 \\ \vdots \\ \tilde{V}_n \end{bmatrix} \tag{1}$$

Where

n is the total number of nodes

Y_{ii} is the self admittance of node i

Y_{ij} is the mutual admittance between nodes i and j

$\tilde{V}_i$ is the phasor voltage to ground at node i

$\tilde{I}_i$ is the phasor current flowing into the network at node i

The set of equations 1 would be linear if $\tilde{I}$ were known, however the current injections are not known for most nodes. The relations between the node currents, P, Q, and V are as follows:

$$\tilde{I}_i = \frac{P_i - jQ_i}{\tilde{V}_i^*} \tag{2}$$

Due to non linearity of the problem, load flow equations are solved iteratively. Several techniques have been developed to solve the set of equations, [16] presents various methods developed over the years.

2.2 Load Flow Analysis Techniques

2.2.1 Gauss-Seidel Method:

This is an iterative approach proposed by Seidel in 1874 (Academy of Science, Munich). The equation 2 is rewritten as follows:

$$\frac{P_i - jQ_i}{\tilde{V_i^*}} = Y_{ii}\tilde{V_i} + \sum_{k=1,k\neq i}^{n} Y_{ik}\tilde{V_k} \tag{3}$$

The voltage $\tilde{V_i}$ may be expressed as

$$\tilde{V_i} = \frac{P_i - jQ_i}{Y_{ii}\tilde{V_i^*}} - \frac{1}{Y_{ii}} \sum_{k=1,k\neq i}^{n} Y_{ik}\tilde{V_k} \tag{4}$$

For a load (PQ) bus, P and Q are know, and equation 4 is used to compute the voltage $\tilde{V_i}$ by using updated voltages as soon as they are available i.e., for the P^{th} iteration, the bus voltages used for computing voltage V_i at bus i are $V_1^p, V_2^p, \ldots, V_{i-1}^p, V_i^{p-1}, V_{i+1}^{p-1}, \ldots, V_n^{p-1}$.

If i^{th} bus is a generator bus, the reactive power to be generated is calculated using equation 5. If the computed Q_i is within the Q limits of the generator, the value is used in equation 4 to compute the updated value of V_i. The value of the voltage is forced to be the specified value by multiplying the real and imaginary parts of the equation 4 with ratio of specified value of the magnitude of generator voltage to the magnitude of its updated value.

$$Q_i = -Im[\tilde{V_i^*} \sum_{k=1}^{n} Y_{ik}\tilde{V_k}] \tag{5}$$

On the other hand, if the computed Q_i exceeds the Q limits of the generator, it is set to the maximum or minimum limit based on whether it is above or below the limits of the generator. The updated $\tilde{V_i}$ is then computed by treating the bus as a PQ bus.

The iterations are continued until the real and imaginary components of voltages at each bus computed by successive iterations converge to a pre specified tolerance. The Gauss-Seidel method has slow convergence because of weak diagonal dominance of the node admittance matrix. Acceleration factors are often used to speed up the convergence:

$$V_k^{\tilde{new}} = V_k^{\tilde{old}} + c(V_k^{\tilde{new}} - V_k^{\tilde{old}}) \tag{6}$$

Where c is the acceleration factor, typically on the order of 1.4 to 1.7.

2.2.2 Newton-Raphson (N-R) Method:

Newton-Raphson method is an iterative technique used for solving a set of non-linear equations. Let equation 7 represent a set of equations with n unknowns:

$$\begin{aligned} f_1(x_1, x_2, \ldots, x_n) &= b_1 \\ f_2(x_1, x_2, \ldots, x_n) &= b_2 \\ f_3(x_1, x_2, \ldots, x_n) &= b_3 \\ &\ldots\ldots\ldots\ldots\ldots\ldots \\ f_n(x_1, x_2, \ldots, x_n) &= b_n \end{aligned} \tag{7}$$

The process stats with an initial guess of all the n unknowns $x_1^0, x_2^0, x_3^0, \ldots, x_n^0$ and if $\Delta x_1, \Delta x_2, \Delta x_3, \ldots, \Delta x_n$ are the corrections necessary to the initial guess so that the equations are exactly satisfied, we have

$$
\begin{aligned}
f_1(x_1^0 + \Delta x_1, x_2^0 + \Delta x_2, \ldots, x_n^0 + \Delta x_n) &= b_1 \\
f_2(x_1^0 + \Delta x_1, x_2^0 + \Delta x_2, \ldots, x_n^0 + \Delta x_n) &= b_2 \\
f_3(x_1^0 + \Delta x_1, x_2^0 + \Delta x_2, \ldots, x_n^0 + \Delta x_n) &= b_3 \\
\ldots \ldots \ldots \ldots \ldots \ldots \ldots \ldots \ldots & \ldots \ldots \\
f_n(x_1^0 + \Delta x_1, x_2^0 + \Delta x_2, \ldots, x_n^0 + \Delta x_n) &= b_n
\end{aligned} \tag{8}
$$

Each of the above equations can be expanded using Taylor's theorem. The expanded form of the i^{th} equation is

$$
\begin{aligned}
f_i(x_1^0 + \Delta x_1, x_2^0 + \Delta x_2, \ldots, x_n^0 + \Delta x_n) = f_i(x_1^0, x_2^0, x_3^0, \ldots, x_n^0,) \\
+ \left(\frac{\delta f_i}{\delta x_1}\right)_0 \Delta x_1 + \left(\frac{\delta f_i}{\delta x_2}\right)_0 \Delta x_2 + \left(\frac{\delta f_i}{\delta x_3}\right)_0 \Delta x_3 + \ldots + \left(\frac{\delta f_i}{\delta x_n}\right)_0 \Delta x_n \\
+ \text{terms with higher powers of } \Delta x_1, \Delta x_2, \Delta x_3, \ldots, \Delta x_n
\end{aligned} \tag{9}
$$

The higher order terms in equation 9 can be ignored if the initial guess is close to the true solution. The resulting linear set of equations in matrix form is

$$
\begin{bmatrix}
b_1 - f_1(x_1^0, x_2^0, x_3^0, \ldots, x_n^0,) \\
b_2 - f_2(x_1^0, x_2^0, x_3^0, \ldots, x_n^0,) \\
b_3 - f_3(x_1^0, x_2^0, x_3^0, \ldots, x_n^0,) \\
\ldots \ldots \ldots \ldots \ldots \ldots \\
b_n - f_n(x_1^0, x_2^0, x_3^0, \ldots, x_n^0,)
\end{bmatrix}
=
\begin{bmatrix}
\left(\frac{\delta f_1}{\delta x_1}\right)_0 & \left(\frac{\delta f_1}{\delta x_2}\right)_0 & \left(\frac{\delta f_1}{\delta x_3}\right)_0 & \cdots & \left(\frac{\delta f_1}{\delta x_n}\right)_0 \\
\left(\frac{\delta f_2}{\delta x_1}\right)_0 & \left(\frac{\delta f_2}{\delta x_2}\right)_0 & \left(\frac{\delta f_2}{\delta x_3}\right)_0 & \cdots & \left(\frac{\delta f_2}{\delta x_n}\right)_0 \\
\left(\frac{\delta f_3}{\delta x_1}\right)_0 & \left(\frac{\delta f_3}{\delta x_2}\right)_0 & \left(\frac{\delta f_3}{\delta x_3}\right)_0 & \cdots & \left(\frac{\delta f_3}{\delta x_n}\right)_0 \\
\ldots & \ldots & \ldots & \ddots & \ldots \\
\left(\frac{\delta f_n}{\delta x_1}\right)_0 & \left(\frac{\delta f_n}{\delta x_2}\right)_0 & \left(\frac{\delta f_n}{\delta x_3}\right)_0 & \cdots & \left(\frac{\delta f_n}{\delta x_n}\right)_0
\end{bmatrix}
\begin{bmatrix}
\Delta x_1 \\ \Delta x_2 \\ \Delta x_3 \\ \vdots \\ \Delta x_n
\end{bmatrix} \tag{10}
$$

Or

$$\Delta f = J\Delta x \tag{11}$$

Where J is referred to as the *Jacobian*. If the estimated $x_1^0, x_2^0, x_3^0, \ldots, x_n^0$ were exact, then Δf and Δx would be zero. However, as $x_1^0, x_2^0, x_3^0, \ldots, x_n^0$ are only estimates, the errors Δf are finite. Equation 10 represents a linear relationship between the errors Δf and the corrections Δx through the Jacobian of the simultaneous equations. A solution for Δx can be obtained by applying any suitable method for the solution of a set of linear equations. Updated values of x are calculated from equation 12

$$x_i^1 = x_i^0 + \Delta x_i \tag{12}$$

The iterations have quadratic convergence and they are carried out until the errors Δf_i are lower than a specified tolerance. The Jacobian has to be recalculated at each step.

2.2.3 Application of the N-R method to power-flow solution:

In order to apply the Newton-Raphson method to power-flow equations, the complex equations represented by equation 3 are rewritten as two real equations in terms of two real variables. For any node i, we have

$$\tilde{S}_i = P_i + jQ_i = \tilde{V}_i \tilde{I}_i^* \tag{13}$$

From equation 1,

$$\tilde{I}_i = \sum_{m=1}^{n} \tilde{Y_{im}} \tilde{V_m} \tag{14}$$

Substituting $\tilde{I}_i$ given by equation 14 in equation 13 yields

$$P_i + jQ_i = \tilde{V}_i \sum_{m=1}^{n} (G_{im} - jB_{im})\tilde{V}_m^* \tag{15}$$

The product of phasors $\tilde{V}_i$ and $\tilde{V}_m^*$ may be expressed as

$$\begin{aligned} \tilde{V}_i\tilde{V}_m^* = (V_i e^{j\theta_i})(V_m e^{j\theta_m}) = V_i V_m e^{j(\theta_i - \theta_m)} = V_i V_m (cos\theta_{im} + jsin\theta_{im}) \\ \text{where}(\theta_{im} = \theta_i - \theta_m) \end{aligned} \tag{16}$$

The expressions for P_i and Q_i may be written as follows:

$$\begin{aligned} P_i &= V_i \sum_{m=1}^{n} (G_{im}V_m cos\theta_{im} + B_{im}V_m sin\theta_{im}) \\ Q_i &= V_i \sum_{m=1}^{n} (G_{im}V_m sin\theta_{im} - B_{im}V_m cos\theta_{im}) \end{aligned} \tag{17}$$

Thus P and Q at each node is represented as a function of voltage magnitude V and angle θ of all nodes.

If the active and reactive powers at each bus are specified, using subscript *sp* to denote specified values, we may write the load flow equation:

$$
\begin{aligned}
P_1(\theta_1, \theta_2, \ldots, \theta_n, V_1, V_2, \ldots, V_n) &= P_1^{sp} \\
P_2(\theta_1, \theta_2, \ldots, \theta_n, V_1, V_2, \ldots, V_n) &= P_2^{sp} \\
\cdots \cdots \cdots \cdots \cdots \cdots \cdots \cdots \cdots \cdots \cdots \\
P_n(\theta_1, \theta_2, \ldots, \theta_n, V_1, V_2, \ldots, V_n) &= P_n^{sp} \\
Q_1(\theta_1, \theta_2, \ldots, \theta_n, V_1, V_2, \ldots, V_n) &= Q_1^{sp} \\
Q_2(\theta_1, \theta_2, \ldots, \theta_n, V_1, V_2, \ldots, V_n) &= Q_2^{sp} \\
\cdots \cdots \cdots \cdots \cdots \cdots \cdots \cdots \cdots \cdots \cdots \\
Q_n(\theta_1, \theta_2, \ldots, \theta_n, V_1, V_2, \ldots, V_n) &= Q_n^{sp}
\end{aligned}
\tag{18}
$$

Following the general procedure described earlier for the application of the N-R method (Equation 10), we have

$$
\begin{bmatrix}
P_1^{sp} - P_1(\theta_1^0, \ldots, \theta_n^0, V_1^0, \ldots, V_n^0) \\
\cdots \cdots \cdots \cdots \cdots \cdots \cdots \cdots \\
P_n^{sp} - P_n(\theta_1^0, \ldots, \theta_n^0, V_1^0, \ldots, V_n^0) \\
Q_1^{sp} - Q_1(\theta_1^0, \ldots, \theta_n^0, V_1^0, \ldots, V_n^0) \\
\cdots \cdots \cdots \cdots \cdots \cdots \cdots \cdots \\
Q_n^{sp} - Q_n(\theta_1^0, \ldots, \theta_n^0, V_1^0, \ldots, V_n^0)
\end{bmatrix}
=
\begin{bmatrix}
\frac{\delta P_1}{\delta \theta_1} & \cdots & \frac{\delta P_1}{\delta \theta_n} & \frac{\delta P_1}{\delta V_1} & \cdots & \frac{\delta P_1}{\delta V_n} \\
\cdots & \cdots & \cdots & \cdots & \cdots & \cdots \\
\frac{\delta P_n}{\delta \theta_1} & \cdots & \frac{\delta P_n}{\delta \theta_n} & \frac{\delta P_n}{\delta V_1} & \cdots & \frac{\delta P_n}{\delta V_n} \\
\frac{\delta Q_1}{\delta \theta_1} & \cdots & \frac{\delta Q_1}{\delta \theta_n} & \frac{\delta Q_1}{\delta V_1} & \cdots & \frac{\delta Q_1}{\delta V_n} \\
\cdots & \cdots & \cdots & \cdots & \cdots & \cdots \\
\frac{\delta Q_n}{\delta \theta_1} & \cdots & \frac{\delta Q_n}{\delta \theta_n} & \frac{\delta Q_n}{\delta V_1} & \cdots & \frac{\delta Q_n}{\delta V_n}
\end{bmatrix}
\begin{bmatrix}
\Delta\theta_1 \\
\vdots \\
\Delta\theta_n \\
\Delta V_1 \\
\vdots \\
\Delta V_n
\end{bmatrix}
\tag{19}
$$

$$
\begin{bmatrix}
\Delta P \\
\Delta Q
\end{bmatrix}
=
\underbrace{\begin{bmatrix}
\frac{\delta P}{\delta \theta} & \frac{\delta P}{\delta V} \\
\frac{\delta Q}{\delta \theta} & \frac{\delta Q}{\delta V}
\end{bmatrix}}_{Jacobian}
\begin{bmatrix}
\Delta\theta \\
\Delta V
\end{bmatrix}
\tag{20}
$$

For a PV bus, only P is specified and the magnitude of V is fixed. Therefore,

terms corresponding to ΔQ and ΔV would be absent for each of the PV buses. Thus the Jacobian would have only one row and one column for each PV bus.

2.2.4 PV Curve Analysis:

The V-P and Q-V characteristics have been widely used for the voltage stability analysis. Figure 1 shows the relation between receiving end voltage and power for load at different power factors.

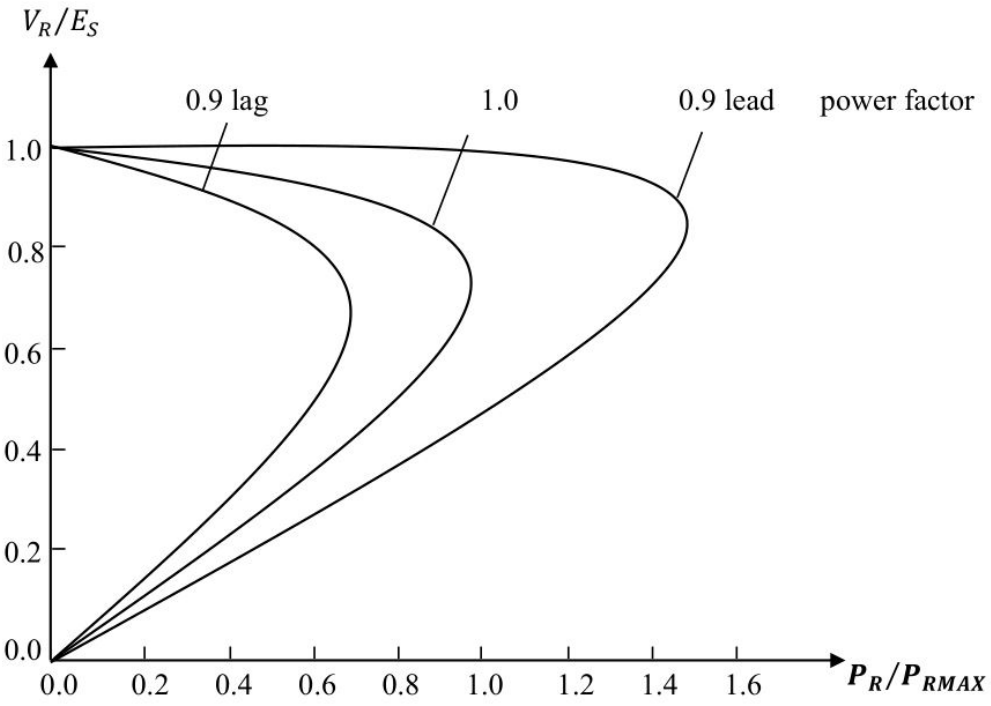

Figure 1: The $V_R - P_R$ characteristics of a power system for different load power factors.

VP characteristic curves are produced by using a series of power flow solutions for different load levels. The analysis involves the increase of P i.e. real power demand in a particular area and voltage magnitude (V) is observed at some critical load buses and then curves for those particular buses will be plotted to determine the voltage stability of a system by static analysis approach.

To explain P-V curve analysis let us assume two-bus system with a single generator, single transmission line and a load, as shown in figure 2.

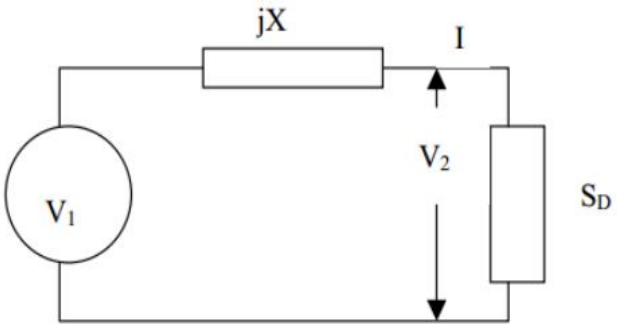

Figure 2: Two bus represetation model.

The complex load assumes the form as shown in equation 21 where V_1 is the sending end voltage and V_2 is the receiving end voltage and $cos\theta$ is the load power factor.

$$S_{12} = P_{12} + jQ_{12} \tag{21}$$

From the Figure 2, the following equations can be derived:

$$\begin{aligned} P_{12} &= |V_1|^2 G - |V_1||V_2|Gcos(\theta_1 - \theta_2) + |V_1||V_2|Bsin(\theta_1 - \theta_2) \\ Q_{12} &= |V_1|^2 B - |V_1||V_2|Bcos(\theta_1 - \theta_2) - |V_1||V_2|Gsin(\theta_1 - \theta_2) \end{aligned} \tag{22}$$

Let G=0, then

$$\begin{aligned} P_{12} &= |V_1||V_2|Bsin(\theta_1 - \theta_2) \\ Q_{12} &= |V_1|^2 B - |V_1||V_2|Bcos(\theta_1 - \theta_2) \end{aligned} \tag{23}$$

The load power is given by,

$$S_D = P_D + jQ_D = -(P_{21} + jQ_{21})$$

$$P_D = -P_{21} = -|V_1||V_2|Bsin(\theta_2 - \theta_1) = |V_1||V_2|Bsin(\theta_1 - \theta_2) \tag{24}$$

$$Q_D = -Q_{21} = -|V_2|^2B - |V_1||V_2|Bcos(\theta_2 - \theta_1) = -|V_2|^2B - |V_1||V_2|Bcos(\theta_1 - \theta_2)$$

Defining $\theta_{12} = \theta_1 - \theta_2$

$$\begin{aligned} P_D &= |V_1||V_2|Bsin\theta_{12} \\ Q_D &= -|V_2|^2B + |V_1||V_2|Bcos\theta_{12} \end{aligned} \tag{25}$$

From the figure, we can also express:

$$\begin{aligned} S_D &= |V_2||I|e^{j\phi} = |V_2||I|(cos\phi + jsin\phi) \\ &= P_D(1 + jtan\phi) = P_D(1 + j\beta), where \beta = tan\phi \\ Q_D &= P_D\beta = -|V_2|^2B + |V_1||V_2|Bcos\theta_{12} \end{aligned} \tag{26}$$

Equating the expressions for P_D and Q_D, we have

$$(|V_2|^2)^2 + \Big[\frac{2P_D\beta}{B} - |V_2|^2 + \frac{P_D}{B^2}[1 + \beta^2]\Big] = 0 \tag{27}$$

Equation 27 is a quadratic in $|V_2|^2$, eliminating θ_{12} and solving the second order equation, we get

$$|V_2|^2 = \frac{1 - \beta P_D \pm \sqrt{[1 - P_D(P_D + 2\beta)]}}{2} \tag{28}$$

As seen in equation 28, the voltage at the load bus is affected by power delivered to the load, the reactance of the line, and power factor of the load. It can be seen that the equation 28 has two solutions for a given set of parameters. One of them corresponds to stable operation and the other corresponds to unstable operation of the system.

In figure 1, the nose of the curve corresponds to the maximum loading point of the system. For a given loading pattern, the PV curves are plotted for selected PQ buses. This reveals the maximum loading margin of the system after which at least one of the bus voltages becomes unstable, which means the system is no longer in stable operating condition. The bus which enters voltage instability first for a given loading pattern can be identified as the weak bus of the system. Installation of reactive compensation devices at such locations can greatly improve the voltage stability and loading margin of the system.

2.2.5 QV Curve Analysis:

Voltage stability is affected considerably by the variations in Q (reactive power consumption) at loads. A more useful characteristic for voltage stability analysis is the Q-V relationship, which shows the sensitivity of bus voltage with respect to reactive power injections and absorptions. A system is voltage stable if V-Q sensitivity is positive for all the buses and is unstable if it is negative for at least one bus.

Figure 3 shows a typical $V_R - Q_R$ characteristic curve of power system.

The base case operating point of the system is represented by the X-intercept of the Q-V curve.

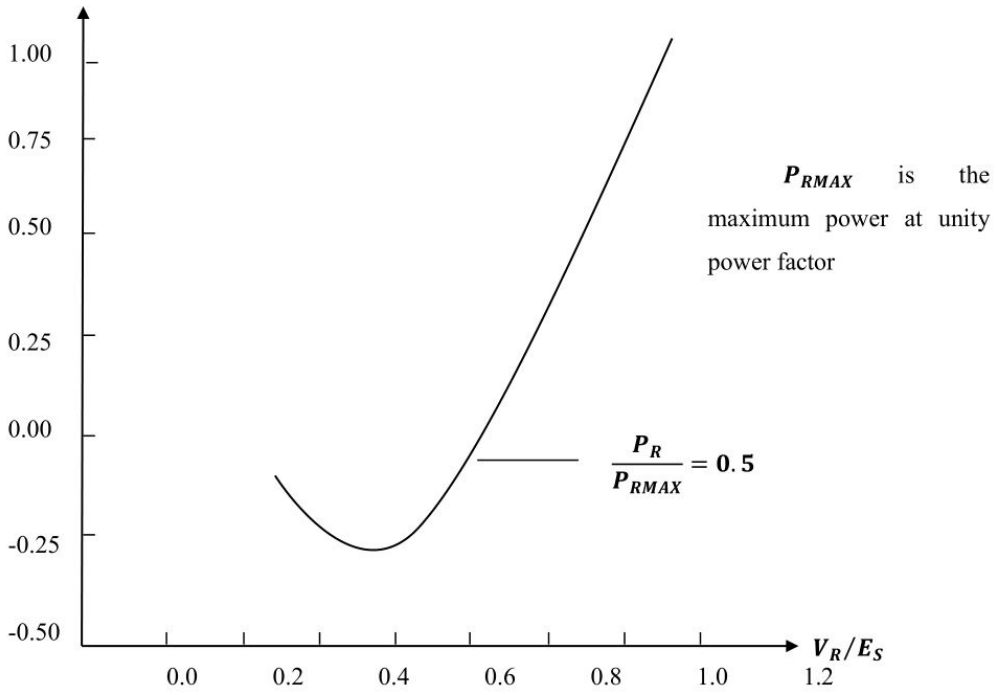

Figure 3: The $V_R - Q_R$ characteristics of a power system.

When a solution is reached using N-R method, we have a linearized model around the given operating point.

$$\begin{bmatrix} J \end{bmatrix} \begin{bmatrix} \Delta\theta \\ \Delta V \end{bmatrix} = \begin{bmatrix} \Delta P \\ \Delta Q \end{bmatrix}$$
$$\text{Where} \quad [J] = \begin{bmatrix} \frac{\delta P}{\delta \theta} & \frac{\delta P}{\delta V} \\ \frac{\delta Q}{\delta \theta} & \frac{\delta Q}{\delta V} \end{bmatrix} \tag{29}$$

The elements of the Jacobian matrix represent the system sensitivity information, i.e., expected small change in bus voltage angle (θ) and voltage magnitude (V) for small changes in P and Q. System voltage stability is affected by both P and Q. In this analysis, at each operating point, P is kept constant and voltage stability is analyzed by considering

the incremental relationship between Q and V. Based on these considerations, in equation 29, let $\Delta P = 0$, we have

$$\begin{gathered} \Delta Q = J_R \Delta V \\ \text{where } J_R = [J_{QV} - J_{Q\theta} J_{P\theta}^{-1} J_{PV}] \end{gathered} \tag{30}$$

Where J_R is the reduced Jacobian matrix. From equation 30, we may write

$$\Delta V = J_R^{-1} \Delta Q \tag{31}$$

The matrix J_R^{-1} is the reduced V-Q Jacobian. Its i^{th} diagonal element is the V-Q sensitivity at bus i. For computational efficiency, the V-Q sensitivities are computed from equation 30.

The V-Q sensitivity of a bus represents the slope of the Q-V curve at the given operating point. A positive V-Q sensitivity is an indicative of stable operation; the smaller the sensitivity, the more stable the system. As stability decreases, the magnitude of the sensitivity increases, becoming infinite at stability limit. A negative V-Q sensitivity however, is an indicative of unstable operation, even a small negative sensitivity represents very unstable operation.

2.2.6 Continuation Load Flow Analysis:

The Jacobian matrix of power flow equations becomes singular at the voltage stability limit. Consequently, conventional power-flow algorithms are prone to convergence problems at operating conditions near the stability limit. Continuation power flow overcomes

this problem. It does so by reformulating the power-flow equations so that they remain well-conditioned at all loading conditions.

The continuation power-flow analysis uses an iterative process involving predictor and corrector steps as depicted in figure 4.

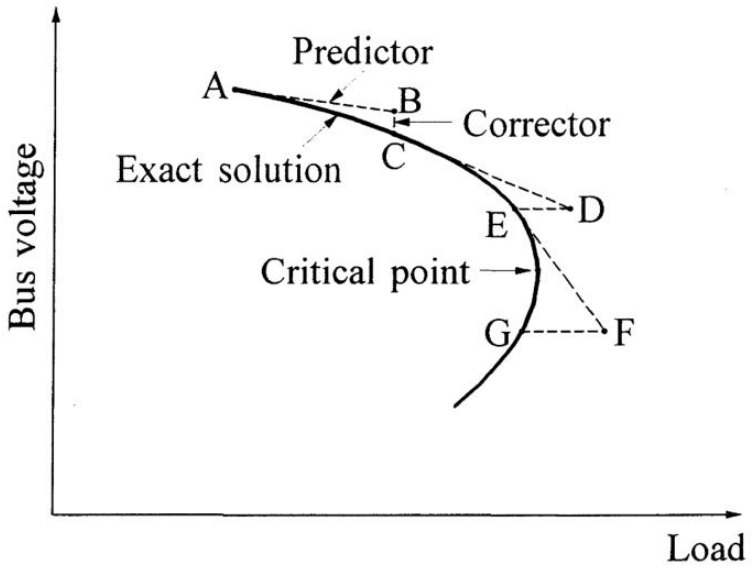

Figure 4: Representation of a typical continuation power-flow process.

From a know initial solution (A), a tangent predictor is used to estimate the solution (B) for a specified patter of load increase. The corrector step then determines the exact solution (C) using a conventional power-flow analysis with system load assumed to be fixed. Successive solutions are obtained by the same predictor and corrector steps. Eventually, the system reaches a loading condition where a corrector step with loads fixed would not converge; therefore, a corrector step with fixed voltage at the monitored bus is applied to find the exact solution (E).

Mathematical Formulation:

The injected powers for i^{th} bus of an n-bus system as represented by equation 17

$$\begin{aligned} P_i &= V_i \sum_{m=1}^{n} (G_{im} V_m cos\theta_{im} + B_{im} V_m sin\theta_{im}) \\ Q_i &= V_i \sum_{m=1}^{n} (G_{im} V_m sin\theta_{im} - B_{im} V_m cos\theta_{im}) \end{aligned} \tag{17}$$

The equations for the real and reactive power injections at bus i are given by equation 32

$$\begin{aligned} P_i &= P_{Gi} - P_{Di} \\ Q_i &= Q_{Gi} - Q_{Di} \end{aligned} \tag{32}$$

The subscript G and D denote generation and demand respectively for bus i.

A load parameter λ is introduced as an additional parameter in equations 32 to simulate load change in the system.

$$\begin{aligned} P_i &= P_{Gi} - (P_{Di} + \lambda(P_{\Delta base})) \\ Q_i &= Q_{Gi} - (Q_{Di} + \lambda(Q_{\Delta base})) \end{aligned} \tag{33}$$

In equation 33, $P_{\Delta base}$ and $Q_{\Delta base}$ are given quantities of powers chosen to scale λ appropriately. The reformulated power-flow equations, with provision for increasing generation as the load is increased may be expressed as follows

$$F(\theta, V) = \lambda K \tag{34}$$

Where

λ is the load parameter

θ is the vector of bus voltage angles

V is the vector of bus voltage magnitudes

K is the vector representing percentage load change at each bus

The equation 34 may be rearranged as equation 35 and is solved by specifying a value for λ as shown in equation 36. Where $\lambda = 0$ represents the base load condition, and $\lambda = \lambda_{critical}$ represents the critical load of the system.

$$F(\theta, V, \lambda) = 0 \tag{35}$$

$$0 \leq \lambda \leq \lambda_{critical} \tag{36}$$

Predictor Step:

To find the solution of the set of equations represented by equation 35, a linear approximation is used by taking an appropriately sized step in direction tangent to the solution path. Therefore, the derivative of equation 35 is taken, which gives

$$F_\theta d\theta + F_V dV + F_\lambda d\lambda = 0$$

$$\text{or} \quad \begin{bmatrix} F_\theta & F_V & F_\lambda \end{bmatrix} \begin{bmatrix} d\theta \\ dV \\ d\lambda \end{bmatrix} = 0 \tag{37}$$

The set of equations 37 have one additional unknown i.e., λ the load parameter. Hence, one more equation is needed to solve these equations. This is satisfied by setting one of the components of the tangent vectors to +1 or -1. This component is referred to as continuation parameter. Setting one of the tangent vector components +1 or -1 imposes a non-zero value on the tangent vector and makes the Jacobian matrix nonsingular at the critical point. With the additional equation, we have

$$\begin{bmatrix} F_\theta & F_V & F_\lambda \\ & e_k & \end{bmatrix} \begin{bmatrix} d\theta \\ dV \\ d\lambda \end{bmatrix} = \begin{bmatrix} 0 \\ \pm 1 \end{bmatrix} \tag{38}$$

Where e_k is the appropriate row vector with all elements equal to zero except the k^{th} element (corresponding to the continuation parameter) begin equal to 1. Initially, the load parameter λ is chosen as the continuation parameter. Subsequently, the parameter with greatest rate of change at a given solution is chosen as the continuation parameter. This is due to the fact that the use of λ as the continuation parameter near critical loading conditions can cause the solution to diverge if the estimate exceeds the maximum load. Conversely, when the voltage magnitude is used as the continuation parameter the solution

may diverge if large steps in voltage change are used. A good practice is to choose the continuation parameter as the state variable that has the greatest rate of change near the given solution. If the parameter is increasing +1 is used, if it is decreasing -1 is used in the tangent vector equation 38.

The tangent vectors can be obtained by solving equation 38. Once these are solved for, the prediction can be made as follows

$$\begin{bmatrix} \theta \\ V \\ \lambda \end{bmatrix}^{p+1} = \begin{bmatrix} \theta \\ V \\ \lambda \end{bmatrix}^{p} + \sigma \begin{bmatrix} d\theta \\ dV \\ d\lambda \end{bmatrix} \tag{39}$$

Where the superscript $p+1$ denotes the next predicted solution. The step size σ is chosen so that the predicted solution is within the radius of the convergence of the corrector. If for a step size the solution could not be found, a smaller step size is chosen.

Corrector Step:

The original set of equations 35 is augmented by one equation that specifies the state variable selected as the continuation parameter. This gives

$$\begin{bmatrix} F(\theta, V, \lambda) \\ x_k - \eta \end{bmatrix} = [0] \tag{40}$$

Where x_k is the state variable chosen as continuation parameter and η is the predicted value of this state variable. Equation 40 can be solved using a slightly modified Newton-Raphson power-flow method.

The continuation power-flow analysis can be continued beyond the critical point and thus obtain solutions corresponding to the lower portion of the V-P curve. It should be noted that the tangent component of λ is positive before the critical point is reached, zero at the critical point, and negative beyond this point. Therefore the sign of $d\lambda$ shows whether the critical point is reached or not.

Sensitivity Information:

In continuation process, the tangent vector proves useful in describing the direction of the solution path. If one looks at the elements of the tangent vector as differential changes in the state variables (dV_i and $d\delta_i$) in response to a differential change in system load ($Cd\lambda$, where C is some constant), the potential for a meaningful sensitivity analysis becomes apparent [12].

It can be observed that the voltage at bus i is affected by load changes at not only itself but at other buses as well. Hence the best method for deciding which bus is nearest to its voltage stability limit is to find the bus with the largest $\frac{dV_i}{dP_{Total}}$, where dP_{Total} is the differential change in active load for the whole system.

Using the reformulated power flow equations, the differential change in active system load is as follows:

$$\begin{aligned} dP_{Total} &= \sum_n dP_{Li} = \sum_n [k_{Li} S_{\Delta Base} cos\psi_i] d\lambda \\ &= [S_{\Delta Base} \sum_n k_{Li} cos\psi_i] d\lambda = Cd\lambda \end{aligned} \tag{41}$$

Thus, the weakes bus would be

$$\begin{aligned} bus j : & \left| \frac{dV_j}{dP_{Total}} \right| \\ = & \left| \frac{dV_j}{Cd\lambda} \right| = max \left[\left| \frac{dV_1}{Cd\lambda} \right|, \left| \frac{dV_2}{Cd\lambda} \right|, \ldots, \left| \frac{dV_n}{Cd\lambda} \right| \right] \end{aligned} \tag{42}$$

Since the value of $Cd\lambda$ is same for each dV element in a given tangent vector, the weakest bus can be identified as the bus with largest dV component.

2.3 Summary

Both the load flow techniques Newton-Raphson method and Continuation load flow method have been discussed in detail. The analysis methods PV curve analysis, QV sensitivity analysis, and Continuation load flow analysis have also been explained in this chapter. In the next chapter, a method of analyzing the improvement in system performance is introduced and it is then applied to various test systems in further chapters. Results are then discussed and conclusions based on these results are drawn in the following chapters.

3 Proposed Analysis Method

This chapter is an overview of the procedure followed for comparative analysis of steady state stability methods used for selecting a weak bus where reactive compensation is placed in order to improve voltage stability and loading margin. Three test systems namely the modified IEEE 14 bus system, the IEEE 30 bus system, and the IEEE 57 bus system are used for simulations. The test systems are subjected to an increase in load at load buses based on the bus participation factors until at least one of the bus voltages reaches 0.85 pu. The systems are then simulated using three different stability analysis methods- PV curve Analysis, Continuation Powe Flow, and QV Sensitivity Analysis. Based on each method's indices, a 'weakest bus' within the system is selected for placement of reactive compensation.

We first need to define the term 'weak bus' as opposed to 'optimal location'. In the context of this paper, the weakest bus is the location that is nearest to experiencing voltage collapse. And the optimal location for installation of reactive compensation is the bus location where a reactive compensation when installed, gives the greatest improvement in loading margin of the system.

Each method used in this thesis identifies a system weak bus based on different indices. The definition of weak bus according to each of the analysis techniques is as follows:

- For PV Curve Analysis, the weak bus would be the one that is closest to turning point or "knee" of the curve. For the purpose of this study, the bus that reaches the lowest allowed voltage first for a given load is identified as the weak bus.
- For QV analysis, the elements of the Jacobian matrix with highest $\frac{dQ}{dV}$ magnitude are

the weakest buses in the system. The elements of the $\frac{\delta Q}{\delta V}$ portion of Jacobian matrix gives the information about the buses most sensitive to changes in Q (reactive power absorption/injection). The i_{th} diagonal element with greatest magnitude implies bus i is most sensitive to Q changes.

- The continuation load flow gives tangent vectors of bus voltage magnitude (dV) and angle ($d\theta$) at each bus for different loading conditions. The bus with greatest magnitude of tangent vector of voltage magnitude for loading condition when one of the bus voltage reaches 0.85 pu is identified as the weakest bus of the system.

Each of the analysis techniques has different indices to identify a weak bus. It is useful to identify which method can give better location for installation of reactive compensation.

A reactive compensation device is installed at each of the locations identified as a weak bus of the system using different analysis techniques and various stability metrics are measured. The optimal location for installation of reactive compensation is obtained by brute-force method. Then the metrics such as loading margin, and differential real and reactive power losses when the reactive compensation is installed at the weak buses identified by the stability methods are compared to the metrics measured when a reactive compensation is installed at the optimal location identified by brute-force. This gives a great insight into which method is able to identify the bus which gives the best results in terms of voltage stability and loading margin improvement of the system, relative to the optimal location.

3.1 Approach

The test system weak bus is identified using the three analysis methods. The maximum loading margin, dP_{loss}, and dQ_{loss} are noted. Then, brute-force method is applied to assess the improvement in system performance when a reactive compensation is placed at different locations using loading margin, dP_{loss}, and dQ_{loss} as the metrics. Comparative analysis is then performed.

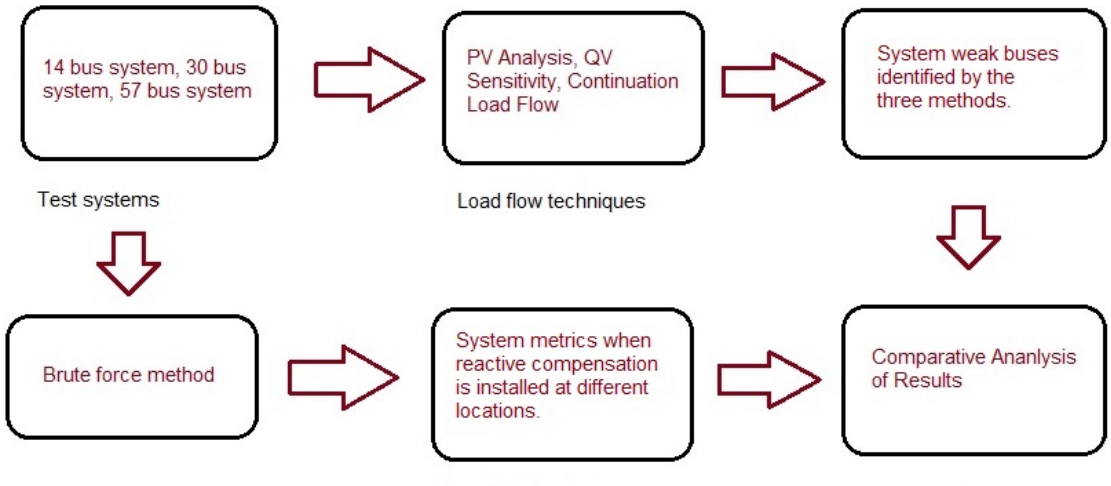

Figure 5: Description of the Approach

3.2 Metrics

The various metrics maximum loading margin, dP_{loss}, and dQ_{loss} used to assess the improvement in system performance are explained in detail below.

- **Maximum Loading Margin:** Maximum Load at which all bus Voltages (V_i where$i \in [1, 2, 3...n]$) $\geq$ 0.85 pu
- $\mathbf{dP_{loss}}$: P_{loss} for max incremental transfer - P_{loss} for base case.

- **dQ_{loss}** : Q_{loss} for max incremental transfer - Q_{loss} for base case.

3.3 4 Step Methodology

A four step methodology has been developed for performing comparative analysis. Figure 6 and Figure 7 show a detailed description of the process followed in this thesis.

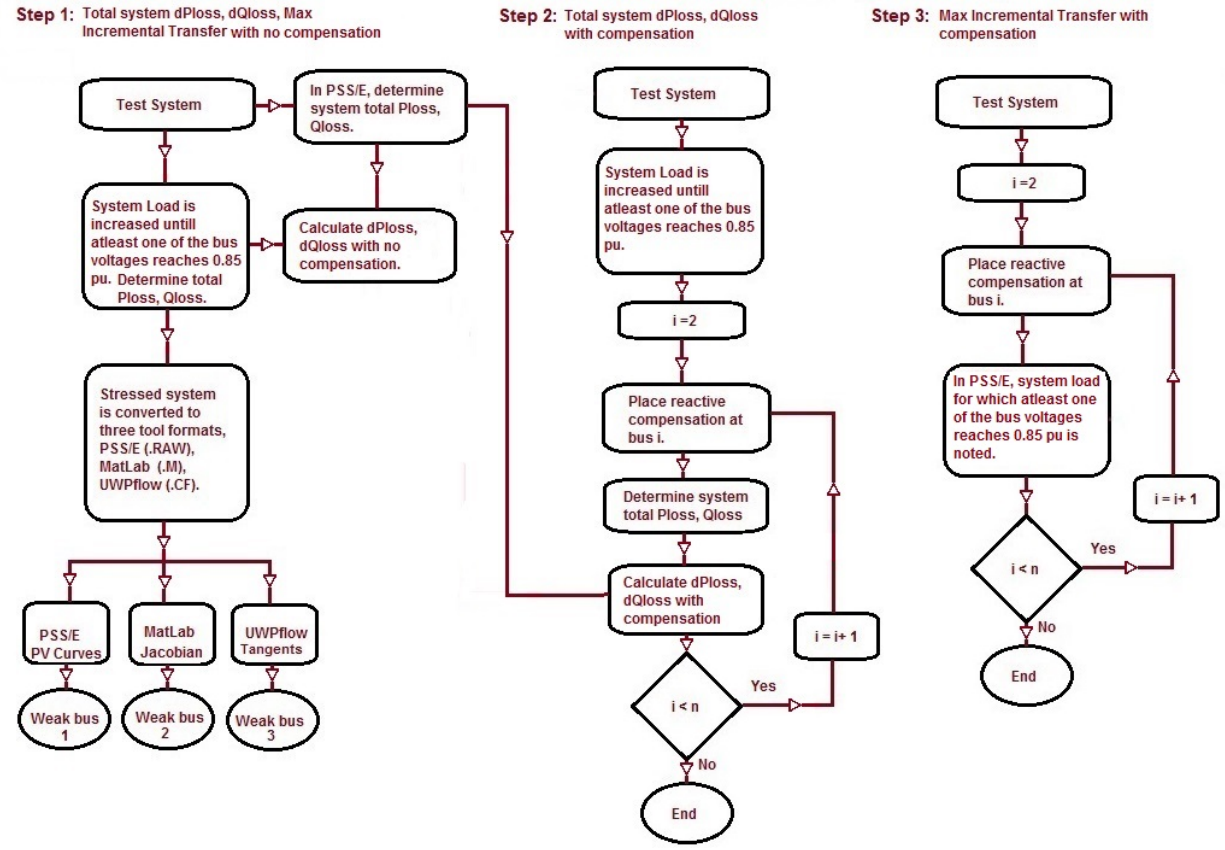

Figure 6: Steps 1, 2, 3

Here, bus 1 is assumed to be the slack bus and is exempted from the study. Hence the placement of reactive compensation begins from bus 2.

First, the test system total real and reactive losses for the base-case load is determined. The system load is then increased until one of the bus voltages reaches 0.85 pu. The increased MW load, along with total system real and reactive losses are determined.

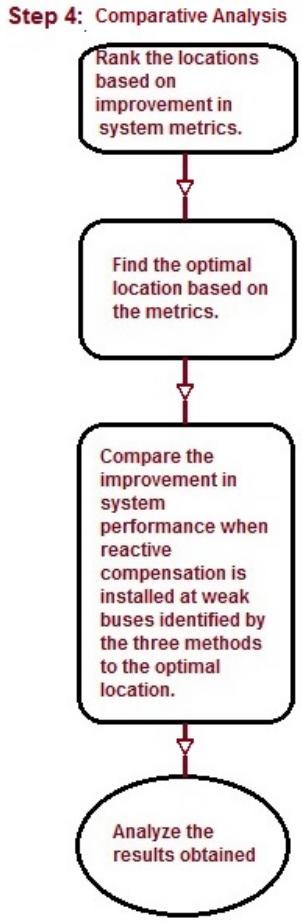

Figure 7: Step 4

The test system with this load is then solved using the three stability methods to identify the system weak buses. The differences in real and reactive losses with the two different loads will give the dP_{loss} and dQ_{loss} for the system with no reactive compensation.

A reactive compensation is then placed on each bus of the test system with the increased load from last step. Corresponding total system P_{loss} and Q_{loss} are determined. The differences between these system losses to those of base-load condition with no reactive compensation will give the new dP_{loss} and dQ_{loss} corresponding to the location where a reactive compensation is placed.

When a reactive compensation is placed at each of the locations, increasing

the load till one of the bus voltage reaches 0.85 pu will reveal the new max load the system can supply. Comparing these values to the maximum loading margin of the system when no reactive compensation is installed will reveal the improvement in system loading margin.

Once the new maximum loading margins, dP_{loss}'s, and dQ_{loss}'s when a reactive compensation is placed at different locations of the system is computed, an optimal location for placement of reactive compensation can be identified based on the improvement in metrics. A comparative analysis can now be performed considering the locations suggested by each method of analysis and the optimal locations.

4 Simulation Tools and Test Systems

For the purpose of simulating three different methods, three applications namely PSS/E for PV curves, Matlab for QV sensitivity, and UWPflow for Continuation Load Flow are used. Three test systems namely the modified IEEE 14 bus system, the IEEE 30 bus system, and the IEEE 57 bus system are used in this thesis.

4.1 Simulation Tools

4.1.1 PSS/E:

The Power System Simulator for Engineering (PSS/E) is a premier software tool owned and distributed by Siemens. Since its introduction in 1976 it has become the most widely used commercial program of its type. PSS/E is a robust tool for analyzing steady state and dynamic performance of a power system. It is an interactive and integrated tool with wide applications including power flow, optimal power flow, balanced and unbalanced fault analysis, dynamic simulation, extended term dynamic simulation, open access and pricing, transfer limit analysis, and network reduction.

4.1.2 Matlab:

MATLAB is a high-level language and interactive environment for numerical computation, visualization, and programming. It includes several built in math functions which enable the user to explore multiple approaches and reach the solution faster than with spreadsheets or traditional programming languages, such as C/C++ or Java. MATLAB can be used for a range of applications, including signal processing and communications, image and video processing, control systems, test and measurement, computational finance,

and computational biology. It is a great tool for data analysis, developing algorithms and creating models, and also features application development.

4.1.3 UWPflow:

UWPflow is a voltage stability analysis program developed by Claudio A. Canizares from the University of Waterloo, Waterloo, Ontario, Canada. The program was developed in C and C++ and has no limitations on system size. It is a research tool designed to calculate local bifurcations related to system limits or singularities in system Jacobian. The program also generates a series of output files that allow further analysis, such as tangent vectors, left and right eigen vectors at a singular bifurcation point, Jacobians, Power flow solutions at different loading levels, and voltage stability indices. The program can be obtained from [17] for educational purposes.

The program can take WSCC/BPA/EPRI formats or IEEE common format as input data format. Additional files such as load and generation change direction files are required for performing a continuation power flow. These files can be obtained from original power flow data and can be user defined. The program also outputs several files in Matlab file format for further analysis.

UWPflow is run by entering commands with options into the command line. This is very similar to unix commands with options. A detailed description of the program along with all the available options can be found in the program manual.

4.2 Test Systems

All the test systems used in this study are obtained in IEEE common data format and converted to other formats as needed.

4.2.1 Modified IEEE 14 Bus System:

The IEEE 14 bus test case represents a portion of the American Electric Power System (in the Midwestern US) as of February, 1962. The 14 bus test case does not have line limits. The system has five PV controlled buses including the slack bus, two with generators and three with synchronous compensators, 11 loads and three transformers. Bus 1 is designated as slack bus of the system. For the purpose of this study, the synchronous compensators at buses 6 and 8 are replaced with generators. The one line diagram and system data were downloaded from [18] and are presented below.

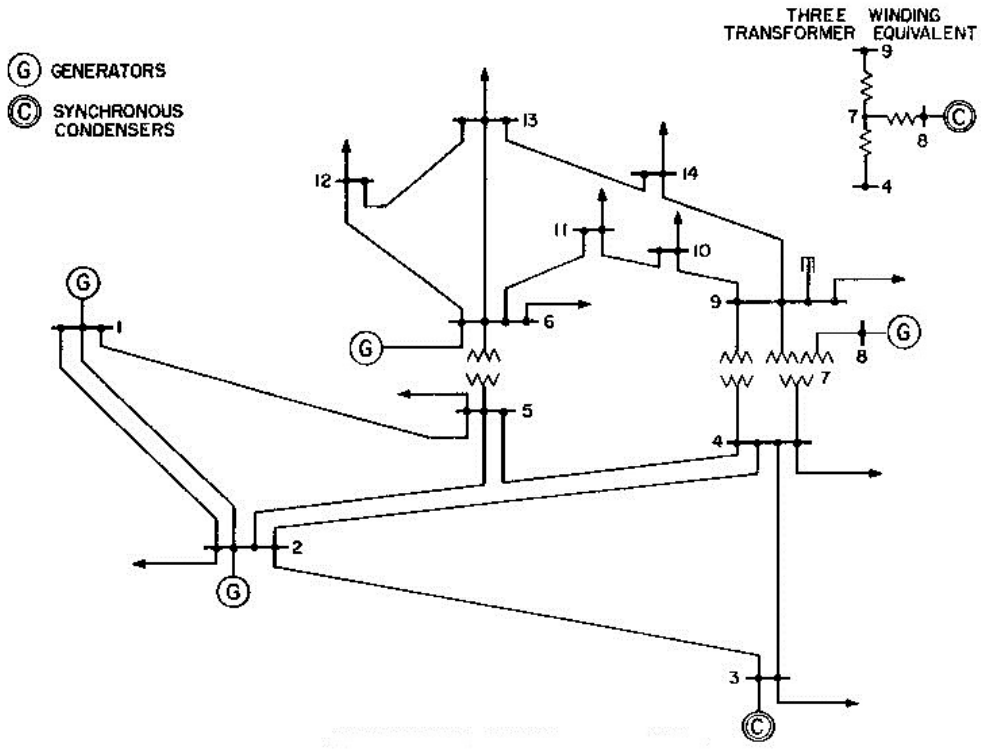

Figure 8: Modified IEEE 14 bus test system.

The bus data and line data of the 14 bus test system are presented in Table 1 and Table 2 respectively.

1	Bus 1	HV	1	1	3	1.06	0	0	0	232.4	-16.9	0	1.06	0	0	0	0	0
2	Bus 2	HV	1	1	2	1.045	-4.98	21.7	12.7	40	42.4	0	1.045	50	-40	0	0	0
3	Bus 3	HV	1	1	2	1.01	-12.72	94.2	19	0	23.4	0	1.01	40	0	0	0	0
4	Bus 4	HV	1	1	0	1.019	-10.33	47.8	-3.9	0	0	0	0	0	0	0	0	0
5	Bus 5	HV	1	1	0	1.02	-8.78	7.6	1.6	0	0	0	0	0	0	0	0	0
6	Bus 6	LV	1	1	2	1.07	-14.22	11.2	7.5	0	12.2	0	1.07	24	-6	0	0	0
7	Bus 7	ZV	1	1	0	1.062	-13.37	0	0	0	0	0	0	0	0	0	0	0
8	Bus 8	TV	1	1	2	1.09	-13.36	0	0	0	17.4	0	1.09	24	-6	0	0	0
9	Bus 9	LV	1	1	0	1.056	-14.94	29.5	16.6	0	0	0	0	0	0	0	0.19	0
10	Bus 10	LV	1	1	0	1.051	-15.1	9	5.8	0	0	0	0	0	0	0	0	0
11	Bus 11	LV	1	1	0	1.057	-14.79	3.5	1.8	0	0	0	0	0	0	0	0	0
12	Bus 12	LV	1	1	0	1.055	-15.07	6.1	1.6	0	0	0	0	0	0	0	0	0
13	Bus 13	LV	1	1	0	1.05	-15.16	13.5	5.8	0	0	0	0	0	0	0	0	0
14	Bus 14	LV	1	1	0	1.036	-16.04	14.9	5	0	0	0	0	0	0	0	0	0

Table 1: Bus data for14 bus test system

1	2	1	1	1 0	0.01938	0.05917	0.0528	0	0	0	0	0	0	0	0	0	0	0
1	5	1	1	1 0	0.05403	0.22304	0.0492	0	0	0	0	0	0	0	0	0	0	0
2	3	1	1	1 0	0.04699	0.19797	0.0438	0	0	0	0	0	0	0	0	0	0	0
2	4	1	1	1 0	0.05811	0.17632	0.034	0	0	0	0	0	0	0	0	0	0	0
2	5	1	1	1 0	0.05695	0.17388	0.0346	0	0	0	0	0	0	0	0	0	0	0
3	4	1	1	1 0	0.06701	0.17103	0.0128	0	0	0	0	0	0	0	0	0	0	0
4	5	1	1	1 0	0.01335	0.04211	0	0	0	0	0	0	0	0	0	0	0	0
4	7	1	1	1 0	0	0.20912	0	0	0	0	0	0	0.978	0	0	0	0	0
4	9	1	1	1 0	0	0.55618	0	0	0	0	0	0	0.969	0	0	0	0	0
5	6	1	1	1 0	0	0.25202	0	0	0	0	0	0	0.932	0	0	0	0	0
6	11	1	1	1 0	0.09498	0.1989	0	0	0	0	0	0	0	0	0	0	0	0
6	12	1	1	1 0	0.12291	0.25581	0	0	0	0	0	0	0	0	0	0	0	0
6	13	1	1	1 0	0.06615	0.13027	0	0	0	0	0	0	0	0	0	0	0	0
7	8	1	1	1 0	0	0.17615	0	0	0	0	0	0	0	0	0	0	0	0
7	9	1	1	1 0	0	0.11001	0	0	0	0	0	0	0	0	0	0	0	0
9	10	1	1	1 0	0.03181	0.0845	0	0	0	0	0	0	0	0	0	0	0	0
9	14	1	1	1 0	0.12711	0.27038	0	0	0	0	0	0	0	0	0	0	0	0
10	11	1	1	1 0	0.08205	0.19207	0	0	0	0	0	0	0	0	0	0	0	0
12	13	1	1	1 0	0.22092	0.19988	0	0	0	0	0	0	0	0	0	0	0	0
13	14	1	1	1 0	0.17093	0.34802	0	0	0	0	0	0	0	0	0	0	0	0

Table 2: Line data for 14 bus test system

4.2.2 IEEE 30 Bus System:

The IEEE 30 bus test case represents a portion of the American Electric Power System (in the Midwestern US) as of December, 1961. Bus 1 (Glen Lyn) is the slack bus of the system. The system has 6 PV controlled buses including the slack bus. It has 4 synchronous compensators and two three winding transformers. There is only one additional generator at bus 2 other than the slack bus. There are 22 buses including bus 2 with loads on them in the system.

The system one line diagram and its bus and line data are obtained from [19] and presented in Figure 9, Table 3, and Table 4 respectively.

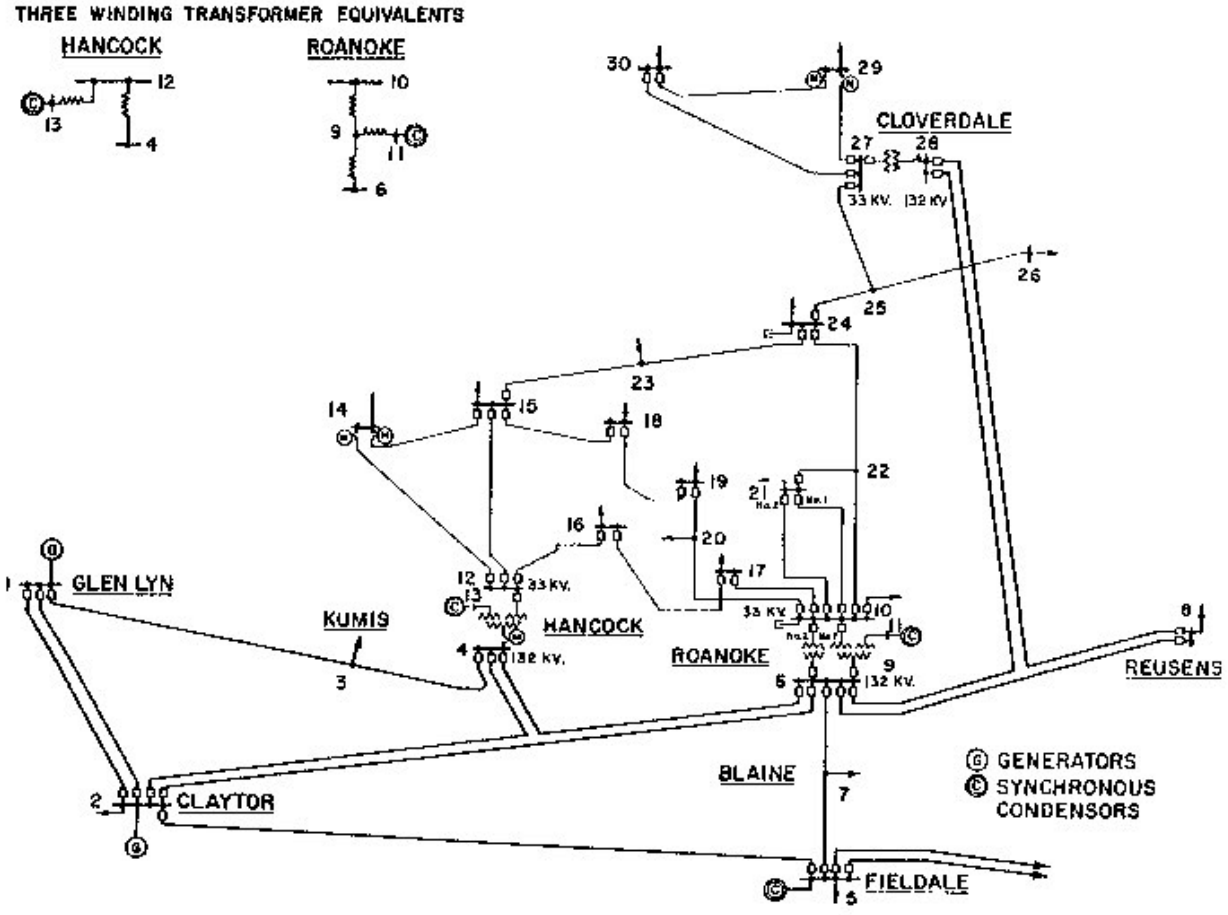

Figure 9: IEEE 30 bus test system.

1	Glen Lyn	132	1	1	3	1.06	0	0	0	260.2	-16.1	132	1.06	0	0	0	0	0
2	Claytor	132	1	1	2	1.043	-5.48	21.7	12.7	40	50	132	1.045	50	-40	0	0	0
3	Kumis	132	1	1	0	1.021	-7.96	2.4	1.2	0	0	132	0	0	0	0	0	0
4	Hancock	132	1	1	0	1.012	-9.62	7.6	1.6	0	0	132	0	0	0	0	0	0
5	Fieldale	132	1	1	2	1.01	-14.37	94.2	19	0	37	132	1.01	40	-40	0	0	0
6	Roanoke	132	1	1	0	1.01	-11.34	0	0	0	0	132	0	0	0	0	0	0
7	Blaine	132	1	1	0	1.002	-13.12	22.8	10.9	0	0	132	0	0	0	0	0	0
8	Reusens	132	1	1	2	1.01	-12.1	30	30	0	37.3	132	1.01	40	-10	0	0	0
9	Roanoke	1	1	1	0	1.051	-14.38	0	0	0	0	1	0	0	0	0	0	0
10	Roanoke	33	1	1	0	1.045	-15.97	5.8	2	0	0	33	0	0	0	0	0.19	0
11	Roanoke	11	1	1	2	1.082	-14.39	0	0	0	16.2	11	1.082	24	-6	0	0	0
12	Hancock	33	1	1	0	1.057	-15.24	11.2	7.5	0	0	33	0	0	0	0	0	0
13	Hancock	11	1	1	2	1.071	-15.24	0	0	0	10.6	11	1.071	24	-6	0	0	0
14	Bus 14	33	1	1	0	1.042	-16.13	6.2	1.6	0	0	33	0	0	0	0	0	0
15	Bus 15	33	1	1	0	1.038	-16.22	8.2	2.5	0	0	33	0	0	0	0	0	0
16	Bus 16	33	1	1	0	1.045	-15.83	3.5	1.8	0	0	33	0	0	0	0	0	0
17	Bus 17	33	1	1	0	1.04	-16.14	9	5.8	0	0	33	0	0	0	0	0	0
18	Bus 18	33	1	1	0	1.028	-16.82	3.2	0.9	0	0	33	0	0	0	0	0	0
19	Bus 19	33	1	1	0	1.026	-17	9.5	3.4	0	0	33	0	0	0	0	0	0
20	Bus 20	33	1	1	0	1.03	-16.8	2.2	0.7	0	0	33	0	0	0	0	0	0
21	Bus 21	33	1	1	0	1.033	-16.42	17.5	11.2	0	0	33	0	0	0	0	0	0
22	Bus 22	33	1	1	0	1.033	-16.41	0	0	0	0	33	0	0	0	0	0	0
23	Bus 23	33	1	1	0	1.027	-16.61	3.2	1.6	0	0	33	0	0	0	0	0	0
24	Bus 24	33	1	1	0	1.021	-16.78	8.7	6.7	0	0	33	0	0	0	0	0.043	0
25	Bus 25	33	1	1	0	1.017	-16.35	0	0	0	0	33	0	0	0	0	0	0
26	Bus 26	33	1	1	0	1	-16.77	3.5	2.3	0	0	33	0	0	0	0	0	0
27	Cloverdle	33	1	1	0	1.023	-15.82	0	0	0	0	33	0	0	0	0	0	0
28	Cloverdle	132	1	1	0	1.007	-11.97	0	0	0	0	132	0	0	0	0	0	0
29	Bus 29	33	1	1	0	1.003	-17.06	2.4	0.9	0	0	33	0	0	0	0	0	0
30	Bus 30	33	1	1	0	0.992	-17.94	10.6	1.9	0	0	33	0	0	0	0	0	0

Table 3: Bus data for IEEE 30 bus test system

1	2	1	1	1	0	0.0192	0.0575	0.0528	0	0	0	0	0	0	0	0	0	0	0	0
1	3	1	1	1	0	0.0452	0.1652	0.0408	0	0	0	0	0	0	0	0	0	0	0	0
2	4	1	1	1	0	0.057	0.1737	0.0368	0	0	0	0	0	0	0	0	0	0	0	0
3	4	1	1	1	0	0.0132	0.0379	0.0084	0	0	0	0	0	0	0	0	0	0	0	0
2	5	1	1	1	0	0.0472	0.1983	0.0418	0	0	0	0	0	0	0	0	0	0	0	0
2	6	1	1	1	0	0.0581	0.1763	0.0374	0	0	0	0	0	0	0	0	0	0	0	0
4	6	1	1	1	0	0.0119	0.0414	0.009	0	0	0	0	0	0	0	0	0	0	0	0
5	7	1	1	1	0	0.046	0.116	0.0204	0	0	0	0	0	0	0	0	0	0	0	0
6	7	1	1	1	0	0.0267	0.082	0.017	0	0	0	0	0	0	0	0	0	0	0	0
6	8	1	1	1	0	0.012	0.042	0.009	0	0	0	0	0	0	0	0	0	0	0	0
6	9	1	1	1	0	0	0.208	0	0	0	0	0	0	0.978	0	0	0	0	0	0
6	10	1	1	1	0	0	0.556	0	0	0	0	0	0	0.969	0	0	0	0	0	0
9	11	1	1	1	0	0	0.208	0	0	0	0	0	0	0	0	0	0	0	0	0
9	10	1	1	1	0	0	0.11	0	0	0	0	0	0	0	0	0	0	0	0	0
4	12	1	1	1	0	0	0.256	0	0	0	0	0	0	0.932	0	0	0	0	0	0
12	13	1	1	1	0	0	0.14	0	0	0	0	0	0	0	0	0	0	0	0	0
12	14	1	1	1	0	0.1231	0.2559	0	0	0	0	0	0	0	0	0	0	0	0	0
12	15	1	1	1	0	0.0662	0.1304	0	0	0	0	0	0	0	0	0	0	0	0	0
12	16	1	1	1	0	0.0945	0.1987	0	0	0	0	0	0	0	0	0	0	0	0	0
14	15	1	1	1	0	0.221	0.1997	0	0	0	0	0	0	0	0	0	0	0	0	0
16	17	1	1	1	0	0.0524	0.1923	0	0	0	0	0	0	0	0	0	0	0	0	0
15	18	1	1	1	0	0.1073	0.2185	0	0	0	0	0	0	0	0	0	0	0	0	0
18	19	1	1	1	0	0.0639	0.1292	0	0	0	0	0	0	0	0	0	0	0	0	0
19	20	1	1	1	0	0.034	0.068	0	0	0	0	0	0	0	0	0	0	0	0	0
10	20	1	1	1	0	0.0936	0.209	0	0	0	0	0	0	0	0	0	0	0	0	0
10	17	1	1	1	0	0.0324	0.0845	0	0	0	0	0	0	0	0	0	0	0	0	0
10	21	1	1	1	0	0.0348	0.0749	0	0	0	0	0	0	0	0	0	0	0	0	0
10	22	1	1	1	0	0.0727	0.1499	0	0	0	0	0	0	0	0	0	0	0	0	0
21	22	1	1	1	0	0.0116	0.0236	0	0	0	0	0	0	0	0	0	0	0	0	0
15	23	1	1	1	0	0.1	0.202	0	0	0	0	0	0	0	0	0	0	0	0	0
22	24	1	1	1	0	0.115	0.179	0	0	0	0	0	0	0	0	0	0	0	0	0
23	24	1	1	1	0	0.132	0.27	0	0	0	0	0	0	0	0	0	0	0	0	0
24	25	1	1	1	0	0.1885	0.3292	0	0	0	0	0	0	0	0	0	0	0	0	0
25	26	1	1	1	0	0.2544	0.38	0	0	0	0	0	0	0	0	0	0	0	0	0
25	27	1	1	1	0	0.1093	0.2087	0	0	0	0	0	0	0	0	0	0	0	0	0
28	27	1	1	1	0	0	0.396	0	0	0	0	0	0	0.968	0	0	0	0	0	0
27	29	1	1	1	0	0.2198	0.4153	0	0	0	0	0	0	0	0	0	0	0	0	0
27	30	1	1	1	0	0.3202	0.6027	0	0	0	0	0	0	0	0	0	0	0	0	0
29	30	1	1	1	0	0.2399	0.4533	0	0	0	0	0	0	0	0	0	0	0	0	0
8	28	1	1	1	0	0.0636	0.2	0.0428	0	0	0	0	0	0	0	0	0	0	0	0
6	28	1	1	1	0	0.0169	0.0599	0.013	0	0	0	0	0	0	0	0	0	0	0	0

Table 4: Line data for IEEE 30 bus test system

4.2.3 IEEE 57 Bus System:

The IEEE 57 bus test system represents a portion of the American Electric Power System (in the Midwestern US) as it was in the early 1960's. Bus 1 (Kanawha) is the slack bus of the system. The system has a total of 7 PV controlled buses including the slack bus. It consists of 3 synchronous compensators and 4 generators including the one at the slack bus.

The system and its bus and line data are obtained from [20] and presented in Figure 10, Table 5, and Table 6 respectively.

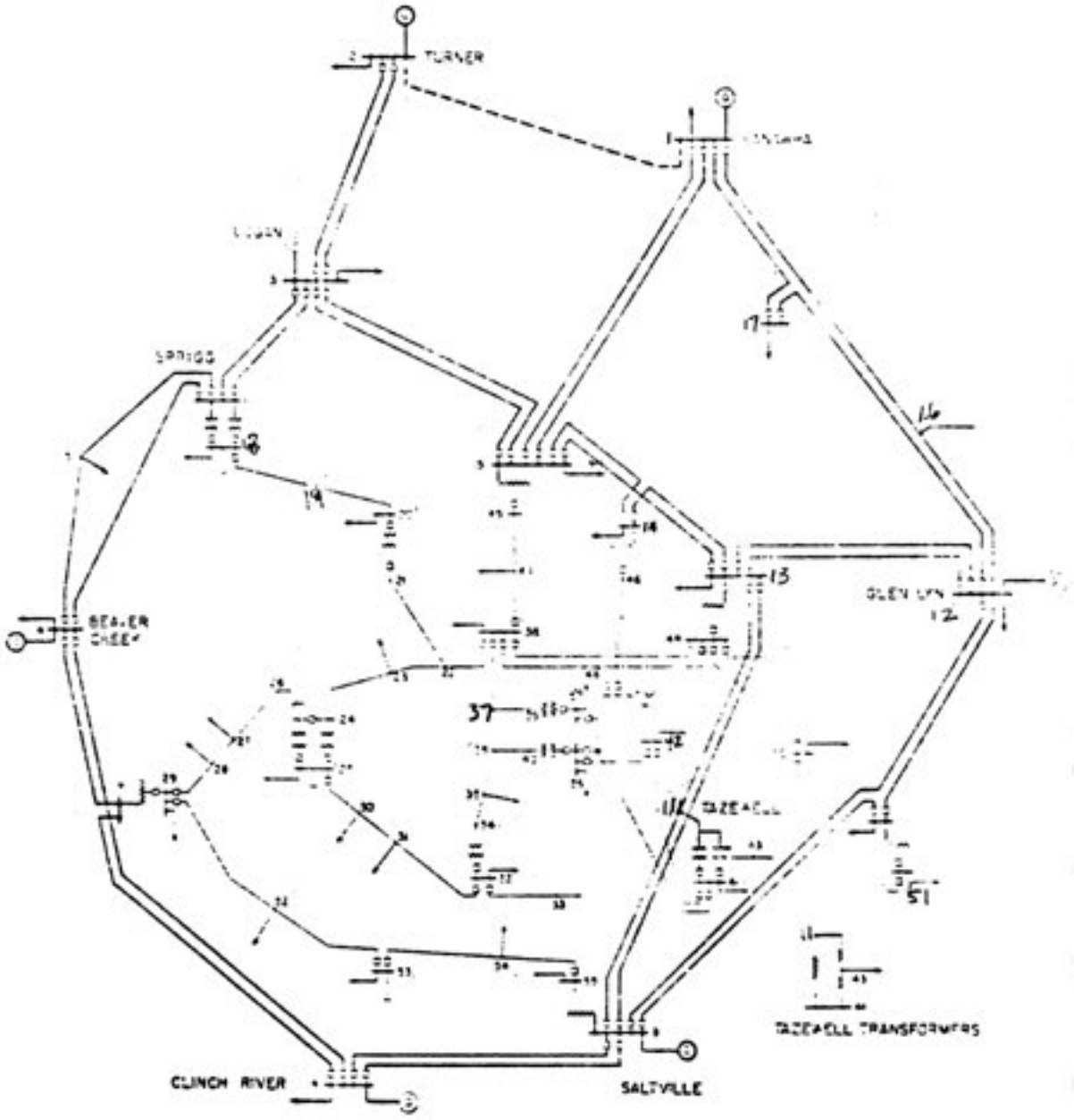

Figure 10: IEEE 57 bus test system.

1	Kanawha	V1	1	1	3	1.04	0	55	17	128.9	-16.1	0	1.04	0	0	0	0	0
2	Turner	V1	1	1	2	1.01	-1.18	3	88	0	-0.8	0	1.01	50	-17	0	0	0
3	Logan	V1	1	1	2	0.985	-5.97	41	21	40	-1	0	0.985	60	-10	0	0	0
4	Sprigg	V1	1	1	0	0.981	-7.32	0	0	0	0	0	0	0	0	0	0	0
5	Bus 5	V1	1	1	0	0.976	-8.52	13	4	0	0	0	0	0	0	0	0	0
6	Beaver Ck	V1	1	1	2	0.98	-8.65	75	2	0	0.8	0	0.98	25	-8	0	0	0
7	Bus 7	V1	1	1	0	0.984	-7.58	0	0	0	0	0	0	0	0	0	0	0
8	Clinch Rv	V1	1	1	2	1.005	-4.45	150	22	450	62.1	0	1.005	200	-140	0	0	0
9	Saltville	V1	1	1	2	0.98	-9.56	121	26	0	2.2	0	0.98	9	-3	0	0	0
10	Bus 10	V1	1	1	0	0.986	-11.43	5	2	0	0	0	0	0	0	0	0	0
11	Tazewell	V1	1	1	0	0.974	-10.17	0	0	0	0	0	0	0	0	0	0	0
12	Glen Lyn	V1	1	1	2	1.015	-10.46	377	24	310	128.5	0	1.015	155	-150	0	0	0
13	Bus 13	V1	1	1	0	0.979	-9.79	18	2.3	0	0	0	0	0	0	0	0	0
14	Bus 14	V1	1	1	0	0.97	-9.33	10.5	5.3	0	0	0	0	0	0	0	0	0
15	Bus 15	V1	1	1	0	0.988	-7.18	22	5	0	0	0	0	0	0	0	0	0
16	Bus 16	V1	1	1	0	1.013	-8.85	43	3	0	0	0	0	0	0	0	0	0
17	Bus 17	V1	1	1	0	1.017	-5.39	42	8	0	0	0	0	0	0	0	0	0
18	Sprigg	V2	1	1	0	1.001	-11.71	27.2	9.8	0	0	0	0	0	0	0	0.1	0
19	Bus 19	V2	1	1	0	0.97	-13.2	3.3	0.6	0	0	0	0	0	0	0	0	0
20	Bus 20	V2	1	1	0	0.964	-13.41	2.3	1	0	0	0	0	0	0	0	0	0
21	Bus 21	V3	1	1	0	1.008	-12.89	0	0	0	0	0	0	0	0	0	0	0
22	Bus 22	V3	1	1	0	1.01	-12.84	0	0	0	0	0	0	0	0	0	0	0
23	Bus 23	V3	1	1	0	1.008	-12.91	6.3	2.1	0	0	0	0	0	0	0	0	0
24	Bus 24	V3	1	1	0	0.999	-13.25	0	0	0	0	0	0	0	0	0	0	0
25	Bus 25	V4	1	1	0	0.982	-18.13	6.3	3.2	0	0	0	0	0	0	0	0.059	0
26	Bus 26	V5	1	1	0	0.959	-12.95	0	0	0	0	0	0	0	0	0	0	0
27	Bus 27	V5	1	1	0	0.982	-11.48	9.3	0.5	0	0	0	0	0	0	0	0	0
28	Bus 28	V5	1	1	0	0.997	-10.45	4.6	2.3	0	0	0	0	0	0	0	0	0
29	Bus 29	V5	1	1	0	1.01	-9.75	17	2.6	0	0	0	0	0	0	0	0	0
30	Bus 30	V4	1	1	0	0.962	-18.68	3.6	1.8	0	0	0	0	0	0	0	0	0
31	Bus 31	V4	1	1	0	0.936	-19.34	5.8	2.9	0	0	0	0	0	0	0	0	0
32	Bus 32	V4	1	1	0	0.949	-18.46	1.6	0.8	0	0	0	0	0	0	0	0	0
33	Bus 33	V4	1	1	0	0.947	-18.5	3.8	1.9	0	0	0	0	0	0	0	0	0
34	Bus 34	V3	1	1	0	0.959	-14.1	0	0	0	0	0	0	0	0	0	0	0
35	Bus 35	V3	1	1	0	0.966	-13.86	6	3	0	0	0	0	0	0	0	0	0
36	Bus 36	V3	1	1	0	0.976	-13.59	0	0	0	0	0	0	0	0	0	0	0
37	Bus 37	V3	1	1	0	0.985	-13.41	0	0	0	0	0	0	0	0	0	0	0
38	Bus 38	V3	1	1	0	1.013	-12.71	14	7	0	0	0	0	0	0	0	0	0
39	Bus 39	V3	1	1	0	0.983	-13.46	0	0	0	0	0	0	0	0	0	0	0
40	Bus 40	V3	1	1	0	0.973	-13.62	0	0	0	0	0	0	0	0	0	0	0
41	Tazewell	V6	1	1	0	0.996	-14.05	6.3	3	0	0	0	0	0	0	0	0	0
42	Bus 42	V6	1	1	0	0.966	-15.5	7.1	4.4	0	0	0	0	0	0	0	0	0
43	Tazewell	V7	1	1	0	1.01	-11.33	2	1	0	0	0	0	0	0	0	0	0
44	Bus 44	V3	1	1	0	1.017	-11.86	12	1.8	0	0	0	0	0	0	0	0	0
45	Bus 45	V3	1	1	0	1.036	-9.25	0	0	0	0	0	0	0	0	0	0	0
46	Bus 46	V3	1	1	0	1.05	-11.89	0	0	0	0	0	0	0	0	0	0	0
47	Bus 47	V3	1	1	0	1.033	-12.49	29.7	11.6	0	0	0	0	0	0	0	0	0
48	Bus 48	V3	1	1	0	1.027	-12.59	0	0	0	0	0	0	0	0	0	0	0
49	Bus 49	V3	1	1	0	1.036	-12.92	18	8.5	0	0	0	0	0	0	0	0	0
50	Bus 50	V3	1	1	0	1.023	-13.39	21	10.5	0	0	0	0	0	0	0	0	0
51	Bus 51	V3	1	1	0	1.052	-12.52	18	5.3	0	0	0	0	0	0	0	0	0
52	Bus 52	V5	1	1	0	0.98	-11.47	4.9	2.2	0	0	0	0	0	0	0	0	0
53	Bus 53	V5	1	1	0	0.971	-12.23	20	10	0	0	0	0	0	0	0	0.063	0
54	Bus 54	V5	1	1	0	0.996	-11.69	4.1	1.4	0	0	0	0	0	0	0	0	0
55	Saltville	V5	1	1	0	1.031	-10.78	6.8	3.4	0	0	0	0	0	0	0	0	0
56	Bus 56	V6	1	1	0	0.968	-16.04	7.6	2.2	0	0	0	0	0	0	0	0	0
57	Bus 57	V6	1	1	0	0.965	-16.56	6.7	2	0	0	0	0	0	0	0	0	0

Table 5: Bus data for IEEE 57 bus test system

1	2	1	1	1	0	0.0083	0.028	0.129	0	0	0	0	0	0	0	0	0	0	0	0
2	3	1	1	1	0	0.0298	0.085	0.0818	0	0	0	0	0	0	0	0	0	0	0	0
3	4	1	1	1	0	0.0112	0.0366	0.038	0	0	0	0	0	0	0	0	0	0	0	0
4	5	1	1	1	0	0.0625	0.132	0.0258	0	0	0	0	0	0	0	0	0	0	0	0
4	6	1	1	1	0	0.043	0.148	0.0348	0	0	0	0	0	0	0	0	0	0	0	0
6	7	1	1	1	0	0.02	0.102	0.0276	0	0	0	0	0	0	0	0	0	0	0	0
6	8	1	1	1	0	0.0339	0.173	0.047	0	0	0	0	0	0	0	0	0	0	0	0
8	9	1	1	1	0	0.0099	0.0505	0.0548	0	0	0	0	0	0	0	0	0	0	0	0
9	10	1	1	1	0	0.0369	0.1679	0.044	0	0	0	0	0	0	0	0	0	0	0	0
9	11	1	1	1	0	0.0258	0.0848	0.0218	0	0	0	0	0	0	0	0	0	0	0	0
9	12	1	1	1	0	0.0648	0.295	0.0772	0	0	0	0	0	0	0	0	0	0	0	0
9	13	1	1	1	0	0.0481	0.158	0.0406	0	0	0	0	0	0	0	0	0	0	0	0
13	14	1	1	1	0	0.0132	0.0434	0.011	0	0	0	0	0	0	0	0	0	0	0	0
13	15	1	1	1	0	0.0269	0.0869	0.023	0	0	0	0	0	0	0	0	0	0	0	0
1	15	1	1	1	0	0.0178	0.091	0.0988	0	0	0	0	0	0	0	0	0	0	0	0
1	16	1	1	1	0	0.0454	0.206	0.0546	0	0	0	0	0	0	0	0	0	0	0	0
1	17	1	1	1	0	0.0238	0.108	0.0286	0	0	0	0	0	0	0	0	0	0	0	0
3	15	1	1	1	0	0.0162	0.053	0.0544	0	0	0	0	0	0	0	0	0	0	0	0
4	18	1	1	1	0	0	0.555	0	0	0	0	0	0	0.97	0	0	0	0	0	0
4	18	1	1	1	0	0	0.43	0	0	0	0	0	0	0.978	0	0	0	0	0	0
5	6	1	1	1	0	0.0302	0.0641	0.0124	0	0	0	0	0	0	0	0	0	0	0	0
7	8	1	1	1	0	0.0139	0.0712	0.0194	0	0	0	0	0	0	0	0	0	0	0	0
10	12	1	1	1	0	0.0277	0.1262	0.0328	0	0	0	0	0	0	0	0	0	0	0	0
11	13	1	1	1	0	0.0223	0.0732	0.0188	0	0	0	0	0	0	0	0	0	0	0	0
12	13	1	1	1	0	0.0178	0.058	0.0604	0	0	0	0	0	0	0	0	0	0	0	0
12	16	1	1	1	0	0.018	0.0813	0.0216	0	0	0	0	0	0	0	0	0	0	0	0
12	17	1	1	1	0	0.0397	0.179	0.0476	0	0	0	0	0	0	0	0	0	0	0	0
14	15	1	1	1	0	0.0171	0.0547	0.0148	0	0	0	0	0	0	0	0	0	0	0	0
18	19	1	1	1	0	0.461	0.685	0	0	0	0	0	0	0	0	0	0	0	0	0
19	20	1	1	1	0	0.283	0.434	0	0	0	0	0	0	0	0	0	0	0	0	0
21	20	1	1	1	0	0	0.7767	0	0	0	0	0	0	1.043	0	0	0	0	0	0
21	22	1	1	1	0	0.0736	0.117	0	0	0	0	0	0	0	0	0	0	0	0	0
22	23	1	1	1	0	0.0099	0.0152	0	0	0	0	0	0	0	0	0	0	0	0	0
23	24	1	1	1	0	0.166	0.256	0.0084	0	0	0	0	0	0	0	0	0	0	0	0
24	25	1	1	1	0	0	1.182	0	0	0	0	0	0	1	0	0	0	0	0	0
24	25	1	1	1	0	0	1.23	0	0	0	0	0	0	1	0	0	0	0	0	0
24	26	1	1	1	0	0	0.0473	0	0	0	0	0	0	1.043	0	0	0	0	0	0
26	27	1	1	1	0	0.165	0.254	0	0	0	0	0	0	0	0	0	0	0	0	0
27	28	1	1	1	0	0.0618	0.0954	0	0	0	0	0	0	0	0	0	0	0	0	0
28	29	1	1	1	0	0.0418	0.0587	0	0	0	0	0	0	0	0	0	0	0	0	0
7	29	1	1	1	0	0	0.0648	0	0	0	0	0	0	0.967	0	0	0	0	0	0
25	30	1	1	1	0	0.135	0.202	0	0	0	0	0	0	0	0	0	0	0	0	0
30	31	1	1	1	0	0.326	0.497	0	0	0	0	0	0	0	0	0	0	0	0	0
31	32	1	1	1	0	0.507	0.755	0	0	0	0	0	0	0	0	0	0	0	0	0
32	33	1	1	1	0	0.0392	0.036	0	0	0	0	0	0	0	0	0	0	0	0	0
34	32	1	1	1	0	0	0.953	0	0	0	0	0	0	0.975	0	0	0	0	0	0
34	35	1	1	1	0	0.052	0.078	0.0032	0	0	0	0	0	0	0	0	0	0	0	0

Table 6: Line data for IEEE 57 bus test system

35	36	1	1	1	0	0.043	0.0537	0.0016	0	0	0	0	0	0	0	0	0	0	0	0
36	37	1	1	1	0	0.029	0.0366	0	0	0	0	0	0	0	0	0	0	0	0	0
37	38	1	1	1	0	0.0651	0.1009	0.002	0	0	0	0	0	0	0	0	0	0	0	0
37	39	1	1	1	0	0.0239	0.0379	0	0	0	0	0	0	0	0	0	0	0	0	0
36	40	1	1	1	0	0.03	0.0466	0	0	0	0	0	0	0	0	0	0	0	0	0
22	38	1	1	1	0	0.0192	0.0295	0	0	0	0	0	0	0	0	0	0	0	0	0
11	41	1	1	1	0	0	0.749	0	0	0	0	0	0	0.955	0	0	0	0	0	0
41	42	1	1	1	0	0.207	0.352	0	0	0	0	0	0	0	0	0	0	0	0	0
41	43	1	1	1	0	0	0.412	0	0	0	0	0	0	0	0	0	0	0	0	0
38	44	1	1	1	0	0.0289	0.0585	0.002	0	0	0	0	0	0	0	0	0	0	0	0
15	45	1	1	1	0	0	0.1042	0	0	0	0	0	0	0.955	0	0	0	0	0	0
14	46	1	1	1	0	0	0.0735	0	0	0	0	0	0	0.9	0	0	0	0	0	0
46	47	1	1	1	0	0.023	0.068	0.0032	0	0	0	0	0	0	0	0	0	0	0	0
47	48	1	1	1	0	0.0182	0.0233	0	0	0	0	0	0	0	0	0	0	0	0	0
48	49	1	1	1	0	0.0834	0.129	0.0048	0	0	0	0	0	0	0	0	0	0	0	0
49	50	1	1	1	0	0.0801	0.128	0	0	0	0	0	0	0	0	0	0	0	0	0
50	51	1	1	1	0	0.1386	0.22	0	0	0	0	0	0	0	0	0	0	0	0	0
10	51	1	1	1	0	0	0.0712	0	0	0	0	0	0	0.93	0	0	0	0	0	0
13	49	1	1	1	0	0	0.191	0	0	0	0	0	0	0.895	0	0	0	0	0	0
29	52	1	1	1	0	0.1442	0.187	0	0	0	0	0	0	0	0	0	0	0	0	0
52	53	1	1	1	0	0.0762	0.0984	0	0	0	0	0	0	0	0	0	0	0	0	0
53	54	1	1	1	0	0.1878	0.232	0	0	0	0	0	0	0	0	0	0	0	0	0
54	55	1	1	1	0	0.1732	0.2265	0	0	0	0	0	0	0	0	0	0	0	0	0
11	43	1	1	1	0	0	0.153	0	0	0	0	0	0	0.958	0	0	0	0	0	0
44	45	1	1	1	0	0.0624	0.1242	0.004	0	0	0	0	0	0	0	0	0	0	0	0
40	56	1	1	1	0	0	1.195	0	0	0	0	0	0	0.958	0	0	0	0	0	0
56	41	1	1	1	0	0.553	0.549	0	0	0	0	0	0	0	0	0	0	0	0	0
56	42	1	1	1	0	0.2125	0.354	0	0	0	0	0	0	0	0	0	0	0	0	0
39	57	1	1	1	0	0	1.355	0	0	0	0	0	0	0.98	0	0	0	0	0	0
57	56	1	1	1	0	0.174	0.26	0	0	0	0	0	0	0	0	0	0	0	0	0
38	49	1	1	1	0	0.115	0.177	0.003	0	0	0	0	0	0	0	0	0	0	0	0
38	48	1	1	1	0	0.0312	0.0482	0	0	0	0	0	0	0	0	0	0	0	0	0
9	55	1	1	1	0	0	0.1205	0	0	0	0	0	0	0.94	0	0	0	0	0	0

Table 7: Continued..Line data for IEEE 57 bus test system

5 Simulations And Results

The proposed method of study to determine the differences in improvement of system performance and identify the stability analysis method that gives the best location for installation of reactive compensation compared to the optimal location identified by brute-force is applied on modified IEEE 14 bus, IEEE 30 bus, and IEEE 57 bus systems. Initially, load flow is performed and the results are compared with other references [14] [18] [19] [20] to ensure validity of the data. The system data are entered in all three tools, PSS/E, Matlab, and UWPflow. Simulations are carried out and the results are presented below:

5.1 Simulations in PSS/E

The test system is built in PSS/E and load flow is performed. Once the load flow converges successfully, the system is stressed until one of the bus voltages reaches 0.85 pu and the PV curves are plotted. Plotting the PV curves of the system reveals the maximum loading margin of the system after which at least one of the bus voltages reaches below pre set minimum value. The total system real power losses (P_{loss}) and reactive power losses (Q_{loss}) for the base load and increased load are noted. The difference between these values referred to in this thesis as the differential real (dP_{loss}) and reactive (dQ_{loss}) losses of the system are calculated. The calculated dP_{loss} and dQ_{loss} correspond to the system with no reactive compensation installed and are expected to improve (reduce) when a reactive compensation is added to the system. The maximum loading margin of the system is noted as well. By observing the PV curve, the weak bus of the system (i.e., the bus that reaches the minimum voltage) is identified.

5.2 Simulations in Matlab

The test system data is provided in a .m file and a program is used to solve for the load flow solution. The system load is increased until one of the bus voltages will reach below the pre set minimum voltage and load flow is carried out at this condition. This reveals the Jacobian matrix of the system for the set of variable (bus voltages, voltage angles, real powers and reactive powers). As discussed in previous chapters, each element of the Jacobian matrix has significant information about the power system. The elements of 4th quadrant of the Jacobian matrix represent the sensitivities of the bus voltages to the reactive power available at the buses. Identifying the bus corresponding to the diagonal element with the greatest magnitude for increased loading condition will reveal the bus that is most sensitive to the reactive power. This according to QV analysis is identified as the system weak bus.

5.3 Simulations in UWPflow

The test system data is provided to the program and solved for the load flow solution using the continuation load flow method. Load flow is stopped when the system load is increased to where one of the bus voltages goes below the pre set minimum voltage. During the process of load flow solution using continuation load flow, tangent vectors of the bus voltage magnitudes and angles are calculated as an integral part of the process. Identifying the bus with tangent vector with greatest magnitude corresponding to voltage magnitude at the increased load will reveal the weakest bus of the system.

Installing a reactive compensation at any of the above identified weak buses

should improve (increase) the system loading margin while all of the bus voltage magnitudes are maintained above the pre-set minimum voltage. The three methods of load flow analysis could lead to three different weak buses in a given test system. A comparison of the improvement in system performance when a reactive compensation is installed at each of the locations suggested by the three stability methods would reveal which location is better compared to others. However, it is possible that there could be another location in the system (i.e., optimal location) where installation of a reactive compensation improves the system performance better than the locations suggested by the three stability methods. For this reason, the reactive compensation is placed at all bus locations in the test system one by one (i.e., brute force) and the corresponding improvement in system performance is recorded and compared to identify the optimal location for placement of reactive compensation based on the metrics.

5.4 Results

Below is a table displaying the maximum incremental transfers, differential real power losses (dP_{loss}), and differential reactive power losses (dQ_{loss}) of the three test systems when no reactive compensation is installed at any of the buses.

System	Max Incremental transfer (MW)	dP_{loss} (MW)	dQ_{loss} (MVAR)
14 bus	185	32.83	127.96
30 bus	105	24.18	93.52
57 bus	190	24.26	99.51

Table 8: Maximum Incremental Transfer (for $V_i \geq 0.85pu$), dP_{loss}, and dQ_{loss} when no reactive compensation in the test systems

A list of the voltages from PV curves, elements of the fourth quadrant of the Jacobian matrix with the greatest magnitude from QV analysis, and tangent vectors corresponding to the voltage magnitudes for the increased load from Continuation Load flow

for each of the test system are presented in the tables below.

Bus	Voltage
14	0.8411
3	0.8906
10	0.8912
8	0.8967
9	0.8994

Table 9: 14 bus system Voltages from PV Curves

Bus	Jacobian Elements
4	32.31
5	30.56
9	18.61
7	16.01
10	11.31

Table 10: 14 bus system Magnitude of Jacobian Elements from QV sensitivity Analysis

Bus	Tangent Vector
14	0.0040809
10	0.0035445
13	0.0034105
9	0.0034006
11	0.0032381

Table 11: 14 bus system greatest magnitude tangent vectors from Continuation Load Flow

Bus	Voltage
30	0.8409
26	0.8519
29	0.8597
25	0.8803
24	0.8834

Table 12: 30 bus system Voltages from PV Curves

Bus	Jacobian Elements
6	75.19
4	51.2
21	40.42
10	38.51
23	36.95

Table 13: 30 bus system Magnitude of Jacobian Elements from QV sensitivity Analysis

Bus	Tangent Vector
19	0.00035921
20	0.0003541
18	0.00034704
23	0.00032977
15	0.00031486

Table 14: 30 bus system greatest magnitude tangent vectors from Continuation Load Flow

Bus	Voltage
31	0.85196
30	0.87619
33	0.88269
32	0.88554
25	0.89734

Table 15: 57 bus system Voltages from PV Curves

Bus	Jacobian Elements
22	76.5
13	70.84
15	64.94
38	63.58
14	52.94

Table 16: 57 bus system Magnitude of Jacobian Elements from QV sensitivity Analysis

Bus	Tangent Vector
31	0.016733
20	0.015963
18	0.015933
23	0.015861
15	0.015368

Table 17: 57 bus system greatest magnitude tangent vectors from Continuation Load Flow

The tables [Table 9-Table 17] show which buses have been identified as weak buses in the test systems by the three load flow analysis methods. According to PV curve analysis, bus 14 is the weakest bus in modified 14 bus system, bus 30 in 30 bus system, and bus 31 in 57 bus system. According to Jacobian sensitivity analysis, bus 4 is the weakest bus in modified 14 bus system, bus 6 in 30 bus system, and bus 22 in 57 bus system. According to Continuation Load Flow analysis, bus 14 is the weakest bus in modified 14 bus system, bus 19 in 30 bus system, and bus 31 in 57 bus system.

Now that a weak bus has been identified in each of the test systems using the three load flow analysis methods, a reactive compensation device can be installed at these locations to compare the improvement in system performance based on the location of installation. The reactive compensation is also installed at all remaining buses one at a time in each of the test system to verify if a better location for of reactive compensation exists and differs from the weak buses identified earlier.

Below are graphs showing the dP_{loss}, dQ_{loss}, maximum incremental transfer, size of reactive compensation resulting in maximum incremental transfer, and the improvement in incremental transfer per unit reactive compensation when a Continuous Controlled Switched Capacitance of 150 MVAR is installed at each of the buses (brute-force method) in all three test systems.

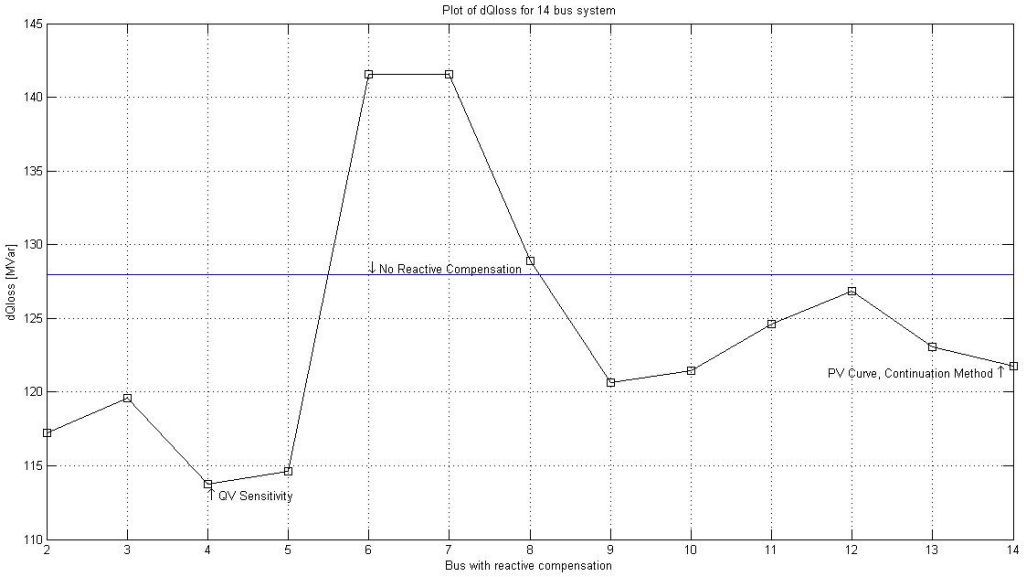

Figure 11: The dQ_{loss} plot of 14 bus system.

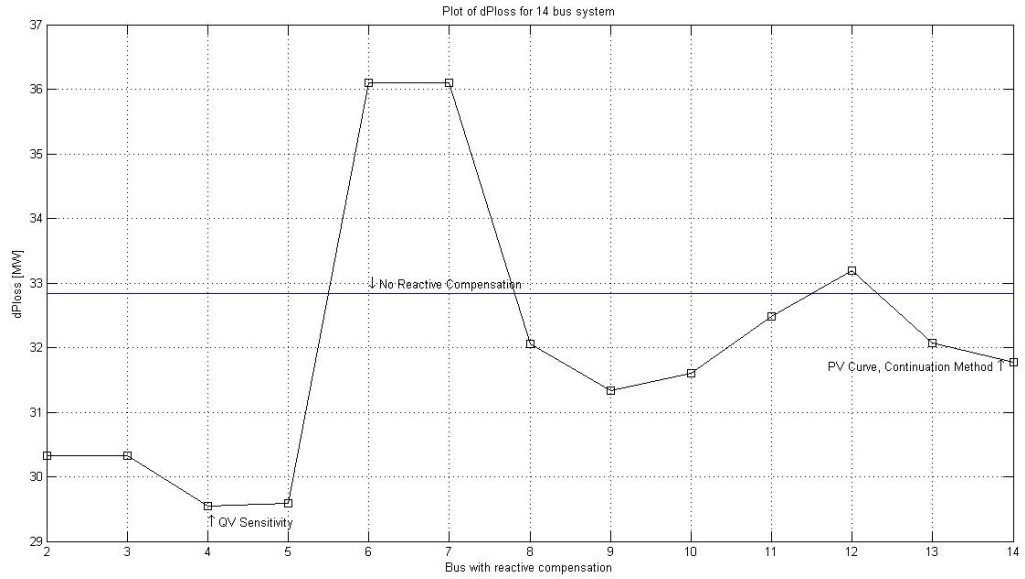

Figure 12: The dP_{loss} plot of 14 bus system.

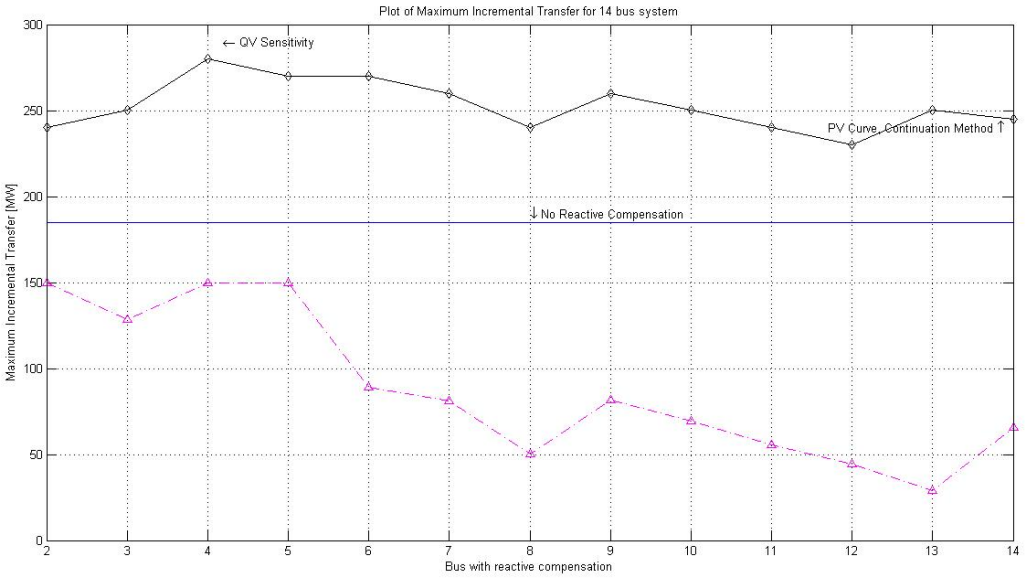

Figure 13: The Maximum Incremental Transfer and size of reactive compensation at Maximum Incremental Transfer of 14 bus system.

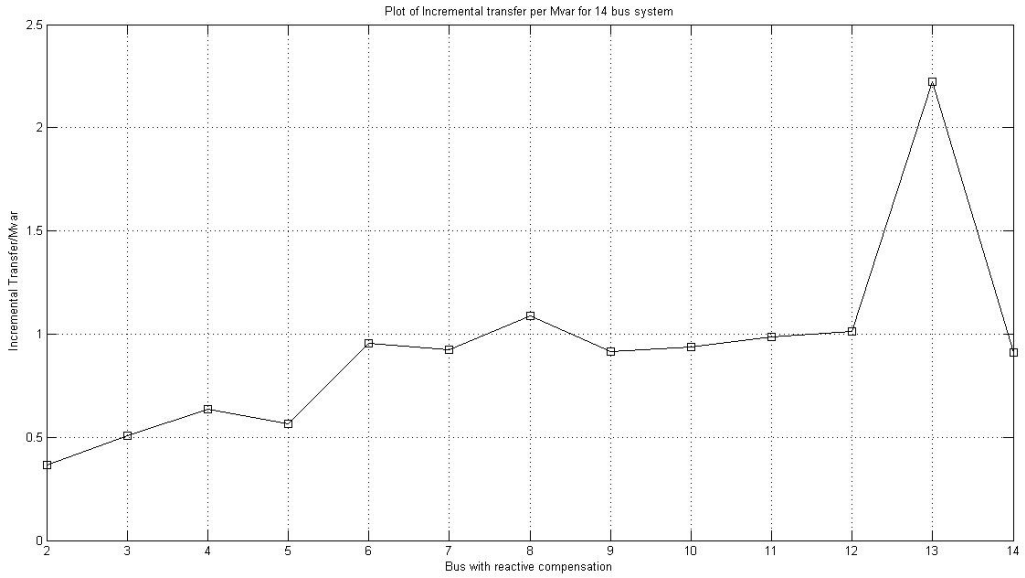

Figure 14: The plot of improvement in Incremental Transfer per unit MVAR in 14 bus system.

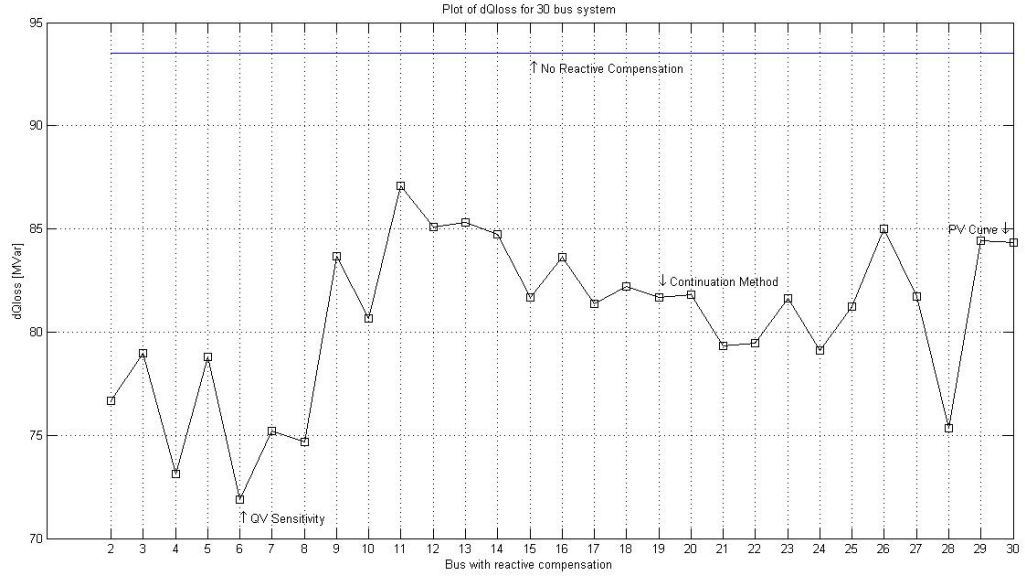

Figure 15: The dQ_{loss} plot of 30 bus system.

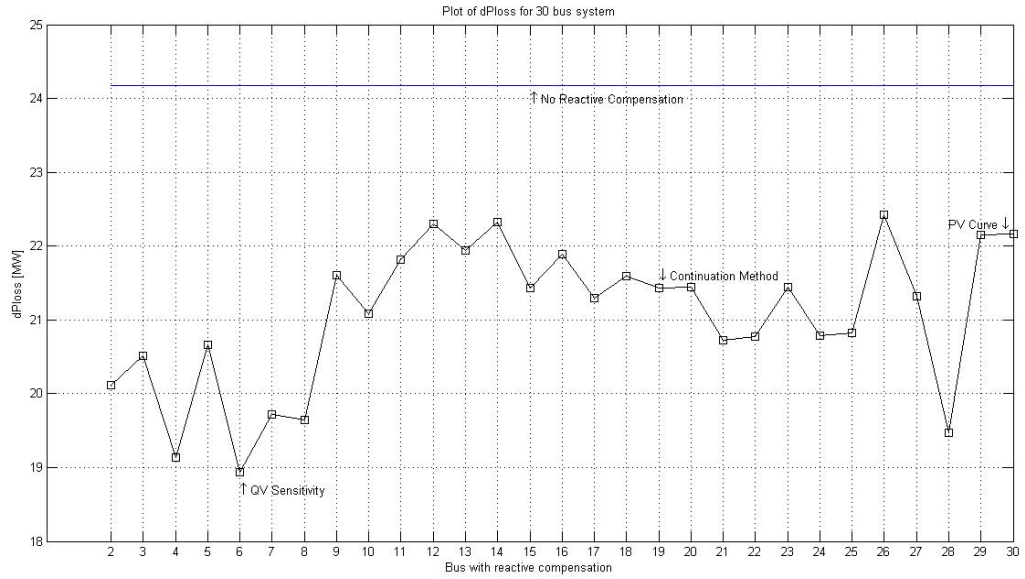

Figure 16: The dP_{loss} plot of 30 bus system.

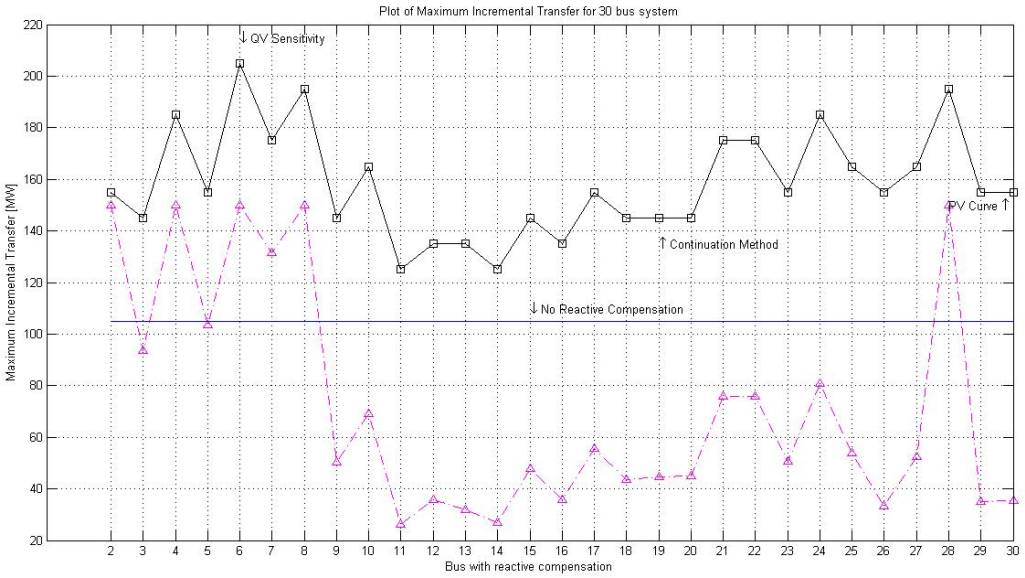

Figure 17: The Maximum Incremental Transfer and size of reactive compensation at Maximum Incremental Transfer of 30 bus system.

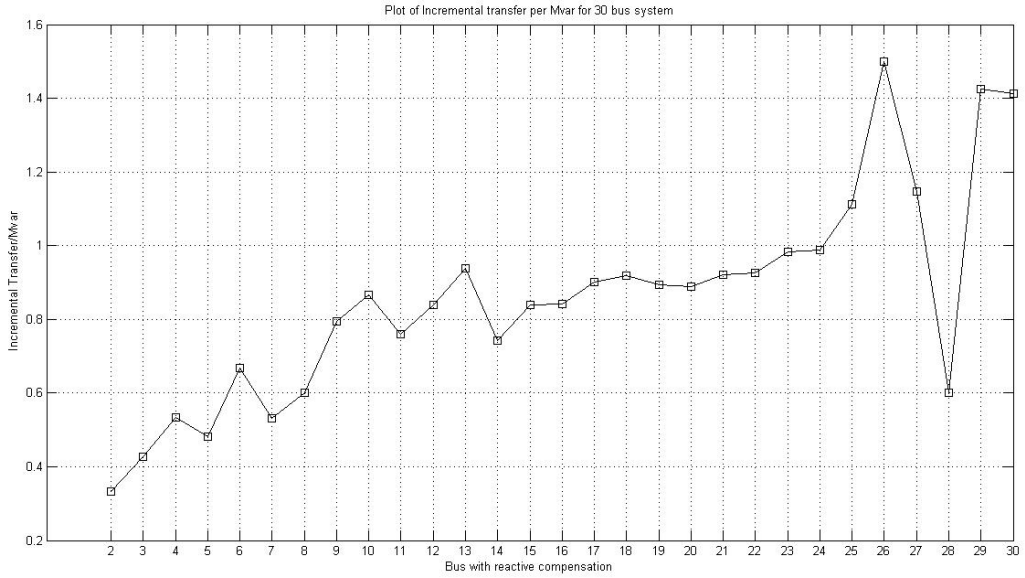

Figure 18: The plot of improvement in Incremental Transfer per unit MVAR in 30 bus system.

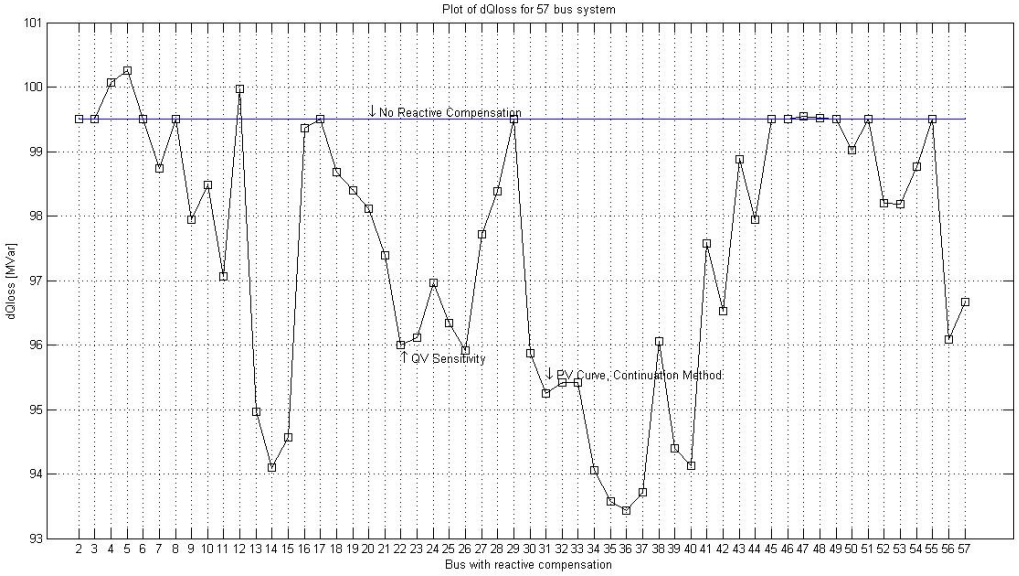

Figure 19: The dQ_{loss} plot of 57 bus system.

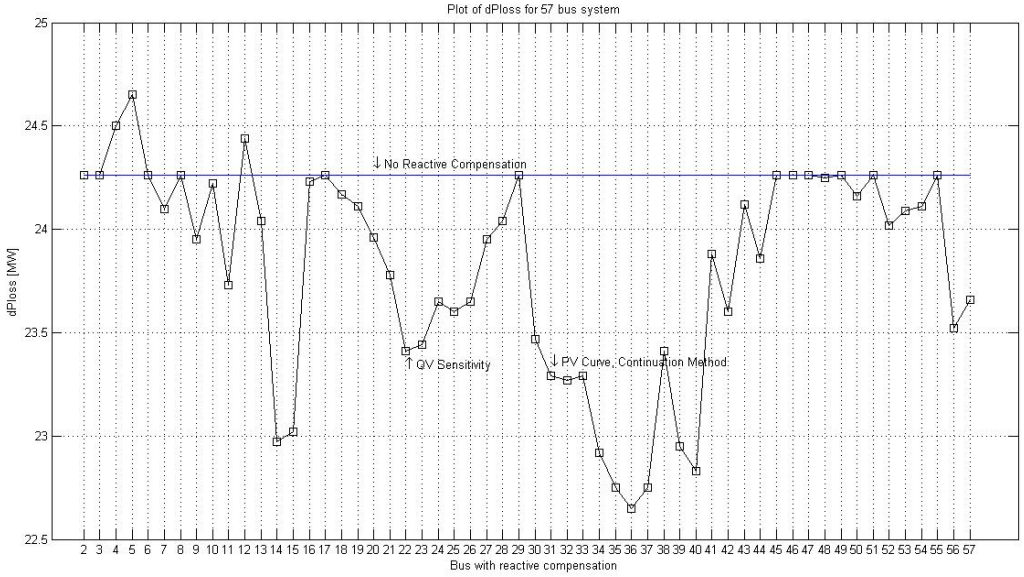

Figure 20: The dP_{loss} plot of 57 bus system.

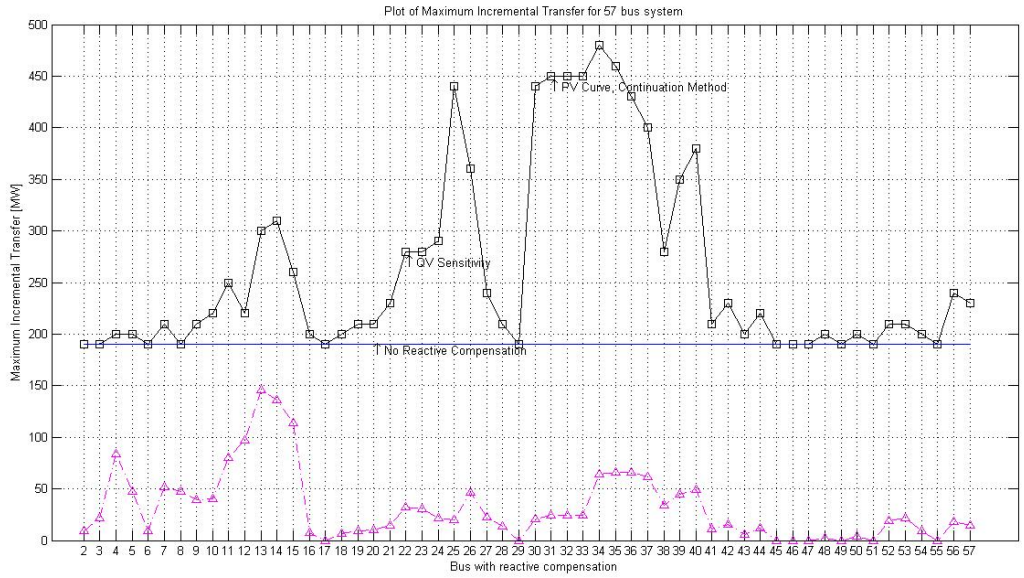

Figure 21: The Maximum Incremental Transfer and size of reactive compensation at Maximum Incremental Transfer of 57 bus system.

System		**Optimal**	PV curves	Continuation Load Flow	Jacobian Sensitivity
14 bus	Bus	**4,4**	14	14	**4**
	dPloss(MW)	**29.55**	31.77	31.77	**29.55**
	dQloss(MVAR)	**113.78**	121.76	121.76	**113.78**
	Max Transfer(MW)	**270**	245	245	**270**
30 bus	Bus	**6,6**	30	19	**6**
	dPloss(MW)	**18.94**	22.19	21.43	**18.94**
	dQloss(MVAR)	**71.88**	84.48	81.7	**71.88**
	Max Transfer(MW)	**205**	135	140	**205**
57 bus	Bus	**36,34**	31	31	22
	dPloss(MW)	**22.72**	23.29	23.29	23.41
	dQloss(MVAR)	**93.35**	95.25	95.25	96
	Max Transfer(MW)	**480**	450	450	280

Table 18: Maximum Incremental Transfer (for $V_i \geq 0.85pu$) for placement of Reactive compensation at weak buses

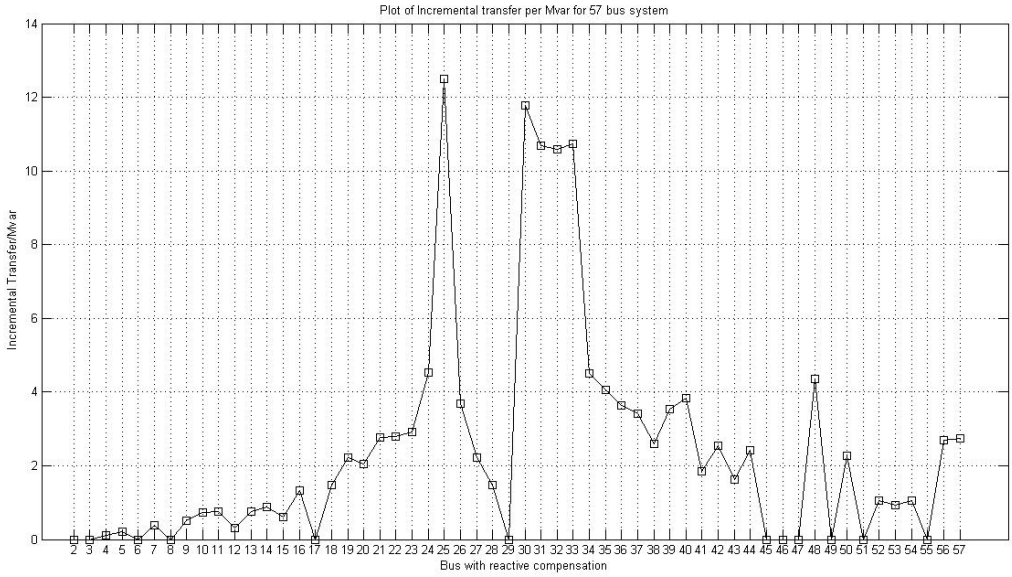

Figure 22: The plot of improvement in Incremental Transfer per unit MVAR in 57 bus system.

The optimal locations for each of the test sytems listed in Table 18 are obtained through brute-force method. A location is deemed as optimal when it yields the greatest improvement in metrics (loading margin, differential real and reactive power losses) of a test system compared to the placement of reactive compensation at any other bus in the system.

In modified 14 bus system, bus 4 is the optimal location for improvement in all three metrics. In 30 bus system, bus 6 is the optimal location for improvement in all three metrics as well. In 57 bus system however, bus 36 is the optimal location for improvement in loading margin and bus 34 is the optimal location for improvement in differential real and reactive power losses (dP_{loss}, dQ_{loss}) of the system. We can now compare these results to the locations suggested by the three stability analysis methods.

The results obtained show that QV sensitivity analysis identified the location where installation of reactive compensation would give the greatest improvement in maximum incremental transfer, dP_{Loss}, and dQ_{Loss} in both modified 14 bus and 30 bus systems. However, in 57 bus system none of the methods identify the location that gives similar results. The location identified by PV curve analysis and Continuation Load Flow in 57 bus system yields close to maximum improvement in loading margin, dP_{Loss}, and dQ_{Loss}. The improvement in system voltage stability can be observed by the decrease in system dQ_{Loss} which plays a key role in system voltage stability. The locations identified as best for installation of reactive compensation also give the best results in terms of voltage stability improvement in both modified 14 bus system and 30 bus system. However, in 57 bus system, the optimal location for installation of reactive power compensation is not the same as the location that gives the best improvement in voltage stability. This leads to different optimal locations for placement of reactive compensation based on the improvement in different metrics.

The plots of improvement in incremental transfer per MVAR present efficiency of installing a reactive compensation at any given location. Based on this, as long as the improvement in metrics meets the requirements, most efficient location of installing a reactive compensation can be chosen to minimize the size of reactive compensation required to meet

the needs.

The results can be better analyzed by classifying the test systems. One way to do this is to classify the systems based on system sparsity. The system sparsity is calculated by dividing the number of non-zero elements (n+2m) to the total number of elements (n^2; where n = number of buses, m = number of branches) in the admittance matrix of the system and then subtracting this from unity. In large-scale power systems, the ratio of number of branches to the number of nodes is about 1.5 [21]. Considering this, the sparsity of such a power system would be (1-0.008 = 0.992) 99.2 % sparse.

Test System	Sparsity
modified 14 bus system	72.5 %
30 bus system	87.8 %
57 bus system	93.4 %

Table 19: Test system sparsity

Figure 23 shows sparsity plot of the three test systems used in this thesis along with a system of 500 nodes and branches to nodes ratio of 1.5. The ratio of number of branches to the number of nodes of the test systems used in thesis is about 1.5. The plot shows that system sparsity increases as the number of nodes in the system increases. In particular, the 57 bus system is the most sparse compared to the modified 14 bus and 30 bus systems.

Based on system sparsity, QV sensitivity method is able to predict the location that gives best results when the system sparsity is 72.5 % and 87.8 %. PV curve analysis and Continuation Load Flow on the other hand perform better when the system sparsity is 93.4 %.

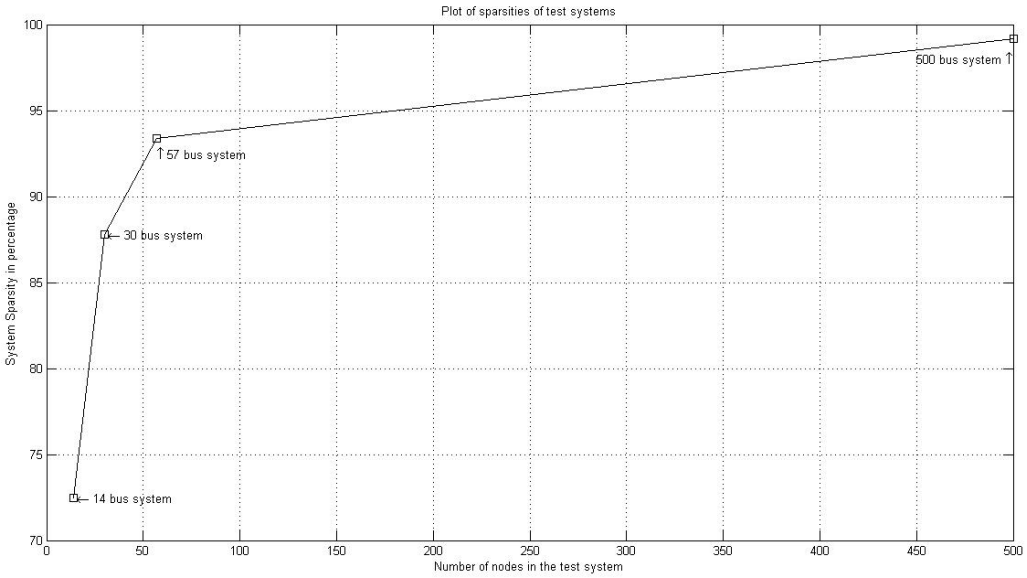

Figure 23: Test system sparsities.

6 Conclusions and Future Work

6.1 Conclusions

The modern power system is under constant stress due to continuously increasing load over the decades. Increasing the maximum loading margin of the system has been an important factor in power system operation and planning. As seen in earlier chapters, reactive power plays a key role in determining the maximum loading of the system. It has also been widely used to improve system loading margin and voltage stability.

The thesis presents a review on the voltage stability analysis along with various major blackouts occurred in recent times. A detailed description of power system analysis methods, PV curves, continuation load flow, and QV sensitivity analysis is presented in chapter 2 along with a detailed explanation of the stability indices obtained in each method used to identify the test system weak bus(es). A 4-step methodology has been developed

to identify the system weak buses using different stability analysis methods, assess the improvement in system performance based on various metrics when a reactive compensation is placed at various locations of the system, and then implement a comparative analysis to identify the method(s) that perform better compared to one another. The test systems are classified to better understand the differences in performances of the analysis methods. The methodology is applied on three test systems, modified IEEE 14 bus system, IEEE 30 bus system, IEEE 57 bus system and results are the presented.

It is observed from the results that each of the methods identify different locations as the best locations for installation of reactive power compensation based on the indices obtained. QV sensitivity analysis successfully identified the best location for installation of reactive power compensation in test systems with sparsity of 72.5 % (modified 14 bus system) and 87.8 % (30 bus system). PV curve analysis and Continuation Load Flow identified the location which provides closer to optimal results in the test system with 93.4 % sparsity (57 bus system).

It can be concluded that the choice of analysis methods could be based on the system topology to obtain the best results. In this thesis system sparsity is used to classify the systems based on which the ideal analysis method can be identified.

6.2 Future Work

As seen in the results, the ideal method of analysis is dependent on the system under consideration. The observations made in this thesis reveal that sparsity could be used as a factor to classify the systems based on which the ideal analysis method can be identified.

To better classify the systems, more test systems with varied sparsity could be used to identify the margin of sparsity for selection of appropriate analysis methods. There

is for example the 118-bus system. Additional metrics such as voltage stability indices proposed by Mohamed [22], Musirin [23], Venikov A [34], Hong Y. H [35], and Zhuo L [36] could be used to assess how close the system is to voltge collapse and could be used as a measure of improvement in system performance. Specifically a reactive compensation would help to decrease the "closeness" to voltage collapse. Other available methods of load flow analysis shall be explored for possible implementation of the methodology proposed in this thesis to determine their performance on different test cases. Last but not least, different system characteristics (other than system sparsity used in this thesis) should be reviewed and could be used to classify the test systems and evaluate the performance of stability analysis methods in identifying the weakest bus. Having used 0.85 p.u. as the minimum voltage level in this study, the author also suggests performing future studies using various voltage levels that might reveal interesting results about the performance of different methods of analysis at different loading levels.

References

[1] P. Kundur, *Power System Stability and Control*, Surrey, British Colombia: McGraw-Hill, Inc. 1994.

[2] Stephen Burnage, *"The US Electric Transmission Grid: Essential infrastructure in need of comprehensive legislation,"*, 2009.

[3] DOE, *"THE SMART GRID: An Introduction"*.

[4] IEEE/CIGRE Joint Task Force on Stability Terms and Definitions, *"Definition and Classification of Power System Stability,"* IEEE TRANSACTIONS ON POWER SYSTEMS, vol.19, no.2, pp. 1387-1401, May. 2004.

[5] C. W. TAYLOR, *Power System Voltage Stabiltiy.* Portland, Oregon: McGraw-Hill, Inc, 1994.

[6] T. Van Cutsem and R. Mailhot, *"Validation of a fast voltage stability analysis methon on Hydro-Qubec System,"* IEEE Trans. Power Systems, Vol. 12, pp. 282-292, Feb. 1997.

[7] J.D. Ainsworth, A. Gavrilovic and H.L. Thanawala, *"Static and Synchronous compensators for HVDC transmission convertors connected to weak systems,"* 28th session CIRGE, pp. 33-01, 1980.

[8] K. Hemmaplardh, J.W. Manke, W. R. Pauly, and J. W. Lamont, *"Considerations for a Long Term Dynamic Simulation Program,"* IEEE Trans, Vol. PWRS-1, pp. 1529-1542, Feb. 1986.

[9] B. Gao, G. K. Morison, and P. Kundur, *"VOLTAGE STABILITY EVALUATION USING MODAL ANALYSIS,"* Transactions on power systems, vol. 7, no. 4, pp. 1529-1542, Nov. 1992.

[10] Galiana. F. D, *"Load Flow Feasibility and the Voltage collapse problem,"* IEEE Proceedings of 23rd conference on Control and Design, pp. 485-487, Dec. 1984.

[11] Tamura.Y, H. Mori, and S. Iwamoto, *"Relationship between voltage instability and multiple load flow solutions in electric power system,"* IEEE Trans. on PAS, no. 5, pp. 1115-1125, May. 1983.

[12] V. Ajjarapu, C. Christy, *"The Continuation Power Flow: A Tool for Steady State Voltage Stability Analysis,"* Power Industry Comoputer Application Conference, pp. 304-311, May. 1991.

[13] S Corsi, G. N. Taranto, *Voltage Instability - The Different Shapes of the "Nose,"* 2007 iREP Symposium - Bulk Power System Dynamics annd Control - VII, Revitalizing Operational Reliability, August. 2007.

[14] A. Sode-Yome, N. Mithulananthan, K.Y. Lee, *"A Comprehensive Comparison of FACTS Devices for Enhancing Static Voltage Stability"* Power Engineering Society General Meeting, IEEE, 2007.

[15] A. Ataputharajah and T. K. Saha, *"Power System Blackouts - Literature Review"* Fourth International Conference on Industrial and Information Systems, pp. 460-465, Dec. 2009.

[16] B. Scott, *"Review of Load-Flow Calculation Methods,"* Proceedings of IEEE, Vol. 62, pp. 916-929, July. 1974.

[17] C. A. Canizares, F. L. Alvarando, and S. Zang, *"UWPflow Program,"* available at "http://www.power.uwaterloo.ca/-claudio/software/pflow.htm", April 2015.

[18] University of Washington, *"IEEE 14 bus test case,"* at "https://www.ee.washington.edu/research/pstca/pf14/pg_tca14bus.htm", April 2015.

[19] University of Washington, *"IEEE 30 bus test case,"* at "https://www.ee.washington.edu/research/pstca/pf30/pg_tca30bus.htm", April 2015.

[20] University of Washington, *"IEEE 57 bus test case,"* at "https://www.ee.washington.edu/research/pstca/pf57/pg_tca57bus.htm", April 2015.

[21] John J. Grainger, William D. Stevenson, Jr. *"Power System Analysis"* International Editions 1994.

[22] A. Mohamed, G.B. Jasmon, and S. Yusoss, *"A Static Voltage Collapse Indicator Using Line Stability Factor"* Journal of Industrial Technology, Vol 7, No. 1. Pt C, pp 73-85, 1989.

[23] Musitin, I.; Rahman, T.K.A., *"Novel fast voltage stability index (FVSI) for voltage stability analysis in power transmission system,"* Research and Development, 2002, SCOReD 2002, Student Conference on, vol., no., pp.265, 268, 2002.

[24] Ana Claudia M. Valle, Geraldo C. Guimaraes, Jose C. de Oliveira, Adelio Jose de Morais *"The Use of Tangent Vectors for Voltage Collapse Analysis,"* International Conference on Electric Utility Deregulation and Restructuring and Power Technologies 2000, City University, London, April 2000.

[25] A. C. M. Valle, G. C. Guimaraes, J. C. de Oliveira, A. J. Morais *"Using Tangent Vectors and Eigenvectors in Power System Voltage Collapse Analysis"* 2001 IEEE Porto Power Tech Conference, Proto, Portugal, September 2001.

[26] B. Isaias Lima Lopes, A. C. Zambroni de Souze, P. Paulo C. Mendes, *"Tangent Vector as a Tool for Voltage Collapse Analysis Considering a Dynamic System Model,"* 2001 IEEE Porto Power Tech Conference, Proto, Portugal, September, 2001.

[27] T. v. Cutsem, C. Vournas, *"Voltage Stability of Electric Power Systems,"* Kluwer Academic Publishers, 1998.

[28] Pablo Guimaraes, Ubaldo Fernandez, Tito Ocariz, Fritz W. Mohn, A. C. Zambroni de Sourza, *"QV and PV curves as a Planning Tool of Analysis,"* 4th International Conference on Electric Utility Deregulation and Restructuring and Power Technologies (DRPT), IEEE conference publications, Pages: 1601-1606, 2011.

[29] M. A. Rios, C. J. zapata, O. Gomez e J. L. Sanchez, *"Voltage Stability assessment with Ranking of Contingencies using QV sensibility,"* IEEE Latin America Transactions, Vol. 7, No. 6, December 2009.

[30] Noor Ropidah Bujal, Amilia Emil Hassan, Marizan Sulaiman, *"Analysis of Voltage Stability Problems in Power System,"* 4th International Conference on Engineering Technology and Technopreneuship (ICE2T), 2014.

[31] Aloui H, Bacha F, Gasmi M, *"Continuation method applied to power system analysis of voltage stability,"* Electrical Machines (ICEM), 2010 XIX International Conference, 2010.

[32] Zhao J, Wang Y, Xu P, *"A comprehensive on-line voltage stability assessment method bsed on continuation power flow,"* Sustainable Power Generation and Supply, 2009 SUPERGEN '09 International Conference, 2009.

[33] Antonio C. Z de Souza, Claudio A. Canizares, Victor H. Quintana, *"New Techniques to speed up Voltage Collapse computations using Tangent Vectors,"* IEEE Transactions on Power Systems, Vol. 12, No. 3, August 1997.

[34] Venikov A, Stroev, V. A, Idelchick V. I, and Tarasov V. I, *"Estimation of electric power system steady-state stability in load flow calculations,"* IEEE Trans. on PAS, Vol. PAS-94, No.3 pp. 1034-1041, May 1975.

[35] Hong Y. H, Pan C. T, and Lin W. W, *"Fast calculation of voltage stability index,"* IEEE Trans. on Power Systems, Vol. 12, No. 4, November 1997.

[36] Zhuo L, *"The impedance analyses of heavy load node in voltage stability studies,"* CSEE Proceedings, Vol. 20, pp: 35-39, April 2000.

Vita

The author was born in 1989, in India. He completed his Bachelors of Engineering degree in Electrical and Electronics Engineering from Osmania University, Hyderabad India in 2010. He finished his Masters in Electrical Engineering from the Univeristy of New Orleans in August 2015. He worked as a Research Assistant with Dr. Parviz Rastgoufard during Masters. His areas of interest are dynamic simulation studies, power systems modeling, voltage stability.